Chapter 2 Distyly in *Nymphoides*

2.1 Introduction

Distyly is defined as a floral dimorphism with a reciprocal arrangement in stigma and anther positions in the floral morphs (Ganders 1979; Dulberger 1992; Lloyd and Webb 1992a). In a distylous population, individual plants produce either short-styled (S-morph) flowers with stigmas positioned below the anthers, or long-styled (L-morph) flowers with stigmas positioned above the anthers. This reciprocal herkogamy is thought to have evolved as an adaptive feature for precise pollen donation and receipt because pollen is deposited onto different parts of a pollinator's body (Darwin 1877; Ganders 1979; Olesen 1979; Barrett 1990; Lloyd and Webb 1992b; Stone and Thomson 1994; Barrett *et al.* 2000; Massinga *et al.* 2005; Armbruster *et al.* 2006). Distylous species also often possess a dimorphic incompatibility system in which only pollination between flowers of different morphs effects seed set (Ganders 1974; Barrett 1990; Barrett *et al.* 2004). Reciprocal herkogamy and incompatibility systems are considered to maintain distyly by promoting efficient cross-pollination but at the same time limiting interference between reproductive organs and therefore, reducing the chances of self-pollination (Webb and Lloyd 1986; Dulberger 1992; Lloyd and Webb 1992b; Barrett 2002a; Cesaro and Thompson 2004).

Since distyly is known as an exceptional example of convergent evolution of floral morphology and incompatibility systems (Ganders 1979), several evolutionary models for distyly have been proposed. The Lloyd-Webb's (1992a; 1992b) pollen-transfer model and Charlesworth-Charlesworth's (1979b) selfing-avoidance model are the two most detailed hypotheses on the evolution of distyly. The two models differ in the selective mechanisms invoked, the ancestral phenotypes and the sequence of establishment of reciprocal herkogamy and incompatibility (Barrett 1990; Barrett 1992c). In the 'pollen-transfer' model, Lloyd and Webb proposed that reciprocal herkogamy evolved prior to self-incompatibility to increase efficient cross-pollination. The initial step in the pathway involved the establishment of stigma-height dimorphism by invasion of a reverse herkogamous morph (stigma positioned below the anthers) into an ancestral population

with approach herkogamous plants (stigma positioned above the anthers). In the second stage of the Lloyd-Webb model for the evolution of distyly, self-incompatibility evolves in response to selfing and inbreeding depression, when most matings occur between the two morphs with stigmas and anthers positioned at reciprocal heights, i.e. disassortative mating. However, in the Charlesworth-Charlesworth's selfing-avoidance model, dimorphic incompatibility evolved in an ancestral population with homostylous plants (stigmas and anthers positioned at the same level), which suffered from self-fertilisation and inbreeding depression. Then, reciprocal herkogamy evolved secondarily to promote the efficiency of pollen transfer between the incompatibility groups.

The Lloyd-Webb model appears to be the more supported evolutionary pathway for distyly. Because most distylous species possess diallelic self-incompatibility, preventing selfing and within morph (intramorph) mating, it appears unlikely that distyly has evolved as a selfing-avoidance mechanism (Lloyd and Webb 1992a; Barrett 2003). Rather, distyly is interpreted as a floral design to achieve mating efficiency through male function by promoting between morph (intermorph) pollen transfer (Lloyd and Webb 1992a; Stone and Thomson 1994; Barrett *et al.* 2000; Barrett 2003; Massinga *et al.* 2005; Pérez-Barrales *et al.* 2006).

Reciprocal herkogamy and incompatibility in distylous species are often accompanied by a balanced morph ratio in populations and a suite of ancillary morphological dimorphisms (Ganders 1979; Barrett 1990; Barrett 1992c; Dulberger 1992; Lloyd and Webb 1992a; Barrett *et al.* 2000; Castro *et al.* 2004; Massinga *et al.* 2005). In distylous species where only fertilisation of the ovules by pollen from a different morph is possible, disassortative mating should lead to an equal morph ratio in populations, i.e. isoplethy (Lloyd and Webb 1992b; Barrett *et al.* 2004; Barrett and Harder 2005). In addition, distylous morphs are also shown to vary in ancillary morphological features, including corolla size, pollen production, pollen size and exine sculpture, and size and morphology of the stigma and stigmatic papillae (Ganders 1979; Dulberger 1992; Lloyd and Webb 1992a; de Castro and Araujo 2004). Recognising these typical features of distyly may be important in evaluating the evolution and maintenance of this breeding system (Faivre and McDade 2001).

Several studies, however, have reported variability in the typical distylous syndrome; the researchers have questioned the evolutionary status of this breeding system; whether

distyly is in a transition process (O'Brien and Calder 1989; Richards and Koptur 1993), or maintained (Faivre and McDade 2001). Atypical distylous species (*sensu* Barrett 1992c) show deviations from the typical morphological and mating patterns of distyly, such as imperfect sex-organ reciprocity (Ornduff 1970c; Opler *et al.* 1975; Riveros *et al.* 1987; Richards and Koptur 1993; Arroyo and Barrett 2000; Massinga *et al.* 2005), variation in the strength of incompatibility systems (Crosby 1949; Bahadur 1966; Bahadur 1970; Ornduff 1970b; Ornduff 1971; Castro *et al.* 2004), unbalanced morph ratios in populations (Crosby 1949; Mulcahy 1964; Levin 1972; Riveros *et al.* 1987; Ornduff 1988; Barrett *et al.* 2004) and lack of differentiation in ancillary traits (Eckert and Barrett 1994b). These atypical features, it has been proposed, result from an unusual association between floral morphology and self-incompatibility systems (Dulberger 1970; Barrett and Harder 2005).

Distyly is the most common breeding system in *Nymphoides* (Ornduff 1988). Two distylous species in the genus, *Nymphoides indica* and *N. humboldtiana*, show typical features of distyly, including floral dimorphism in anther and stigma heights, pollen grain size dimorphism and a strong incompatibility system (Ornduff 1966). An equal morph ratio in a population of *N. indica* suggests disassortative mating governed by strong self-incompatibility (Barrett 1980a). Atypical distylous species are also reported in different Menyanthaceae, including species of *Nymphoides* (Ornduff 1966), *Villarsia* (Ornduff 1988) and *Menyanthes* (Thompson *et al.* 1998). Ornduff (1966) found the high frequency of self- and intramorph pollinations results in either L- or S-biased morph ratios in populations of *Nymphoides peltata*. He suggested that imperfect reciprocity and biased morph ratios do not promote cross-pollinations in *N. peltata* and may lead to breakdown of distyly. In contrast, Thompson *et al.* (1998) reported successful cross-pollination in *Menyanthes trifoliata* despite weak reciprocity between floral morphs. Elsewhere, Ornduff (1988) suggested that intramorph compatibility of S-morphs of *Villarsia parnassiifolia* may bias population morph ratio toward a greater abundance of S-morph plants.

2.2 Aims

In this chapter, the reproductive biology of distylous *Nymphoides montana* is studied to explore the compatibility relations and morphological variations in L-morph and S-morph flowers. The following questions are addressed:

1) What are the frequencies of floral morphs in the natural populations?

2) Does *N. montana* reproduce successfully in its natural habitat?

3) Does *N. montana* show clear sex-organ reciprocity; if not, what floral traits reduce reciprocity?

4) Does *N. montana* show between-morph variation in ancillary dimorphic traits?

5) Does *N. montana* exhibit a diallelic incompatibility system; if so, to what extent?

2.3 Material and Methods

2.3.1 Study species

Nymphoides montana Aston is a perennial aquatic herb (cover image) endemic to Australia (Jacobs 1992). Its distribution is limited to areas of New South Wales, Queensland, South Australia and Victoria (Australia's Virtual Herbarium). Plants reproduce vegetatively by clonal fragmentation (stolon spreading and broken leaves) and sexually by seeds. Each individual plant produces two types of emergent or floating shoots: reproductive shoots with pairs of floral buds at each node and vegetative shoots with newly grown roots and leaves (personal observations). The leaves are cordate. The floral buds develop under water and emerge at anthesis. The five-part flowers open in the morning and close by late afternoon. The yellow petals are fused to form a floral tube with a transverse row of hairs surrounding the petal edges to form a corona at the throat of the floral tube (Figure 2.1). The stamens are epipetalous and are attached to the floral tube. The ovary is superior, 2-carpelate and fused to from a single locule; placentation is parietal. The fruit is a capsule with shiny black, minute seeds ($\leq$ 1.5 mm).

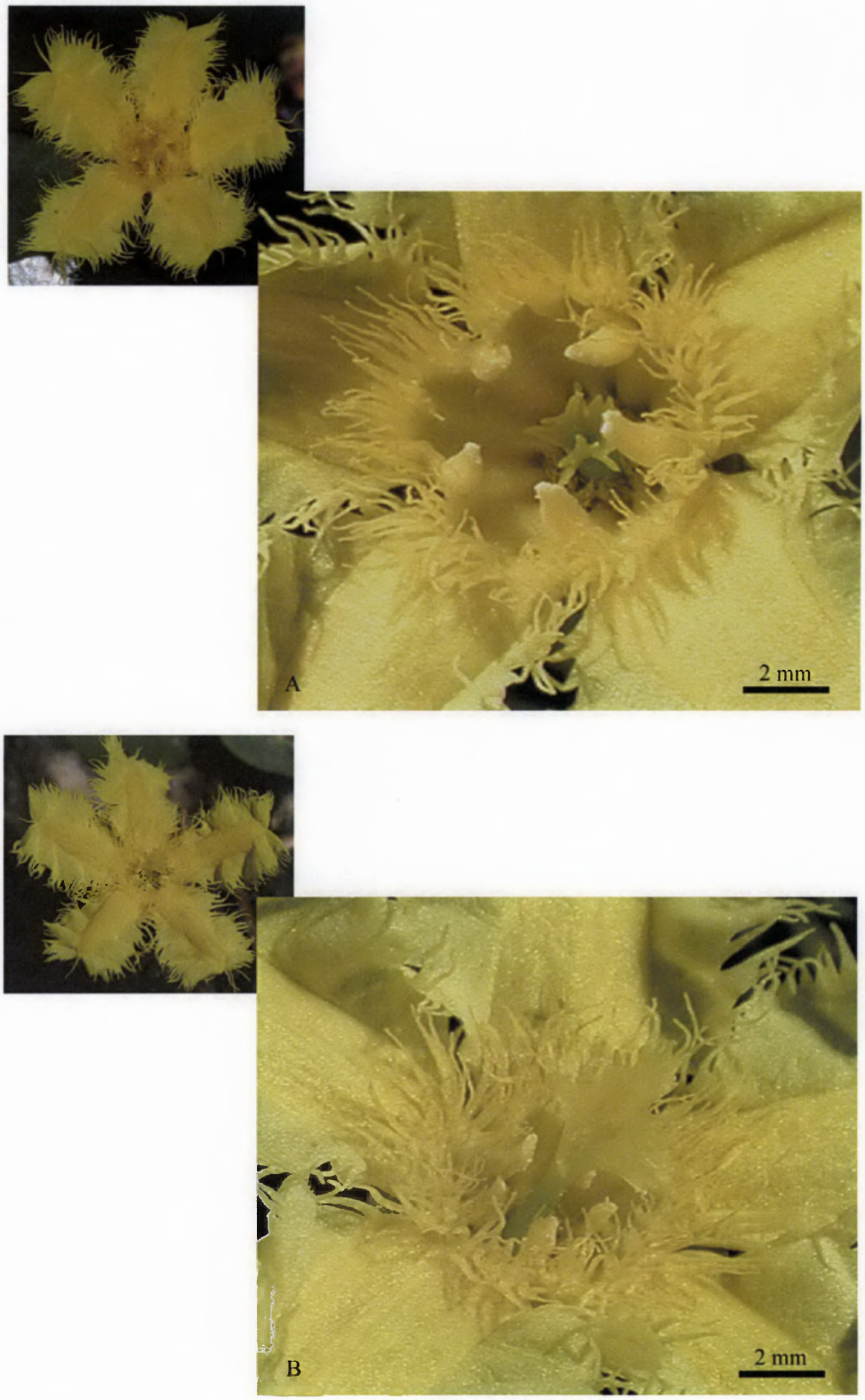

Figure 2.1. Photographs of the distylous *Nymphoides montana* showing the number of flower parts and the disposition of hairs surrounding the petal edges and the corolla tubes of the two floral morphs: A) S-morph and B) L-morph.

2.3.2 Study sites

All study populations were distributed in the Northern Tablelands of New South Wales, Australia: Dumaresq Dam (Figure 2.2; DD, 1070 m elevation; 30° 25′ 48″ S, 151° 35′ 50″ E), Thomas Lagoon (TL, 1035 m elevation; 30° 32′ 43″ S, 151° 33′ 10″ E) and Glencoe (GC, 1150 m elevation; 29° 55′ 30″ S, 151° 43′ 17″ E). The study sites are located at the northern edge of the species' distribution range (Australia's Virtual Herbarium, viewed at 10 September 2007). Plants grow in shallow water on the edges of wetlands. These three populations were chosen since they possess large numbers of individuals in this region. The wetlands differ substantially in water availability. The DD population is in a permanent man-made water body, whereas the TL and GC populations are both naturally occurring and subject to partial flooding with seasonal rainfall. Flowering occurs from mid-spring to late-summer (October-March), a period characterised by warm temperatures and frequent rainfall. At the study sites, native bees were observed to be the most common floral visitors. Other floral visitors included introduced honeybees, e.g. the European honeybee, *Apis mellifera* L., hoverflies (order Diptera) and the occasional butterflies (order Lepidoptera) (Figure 2.3).

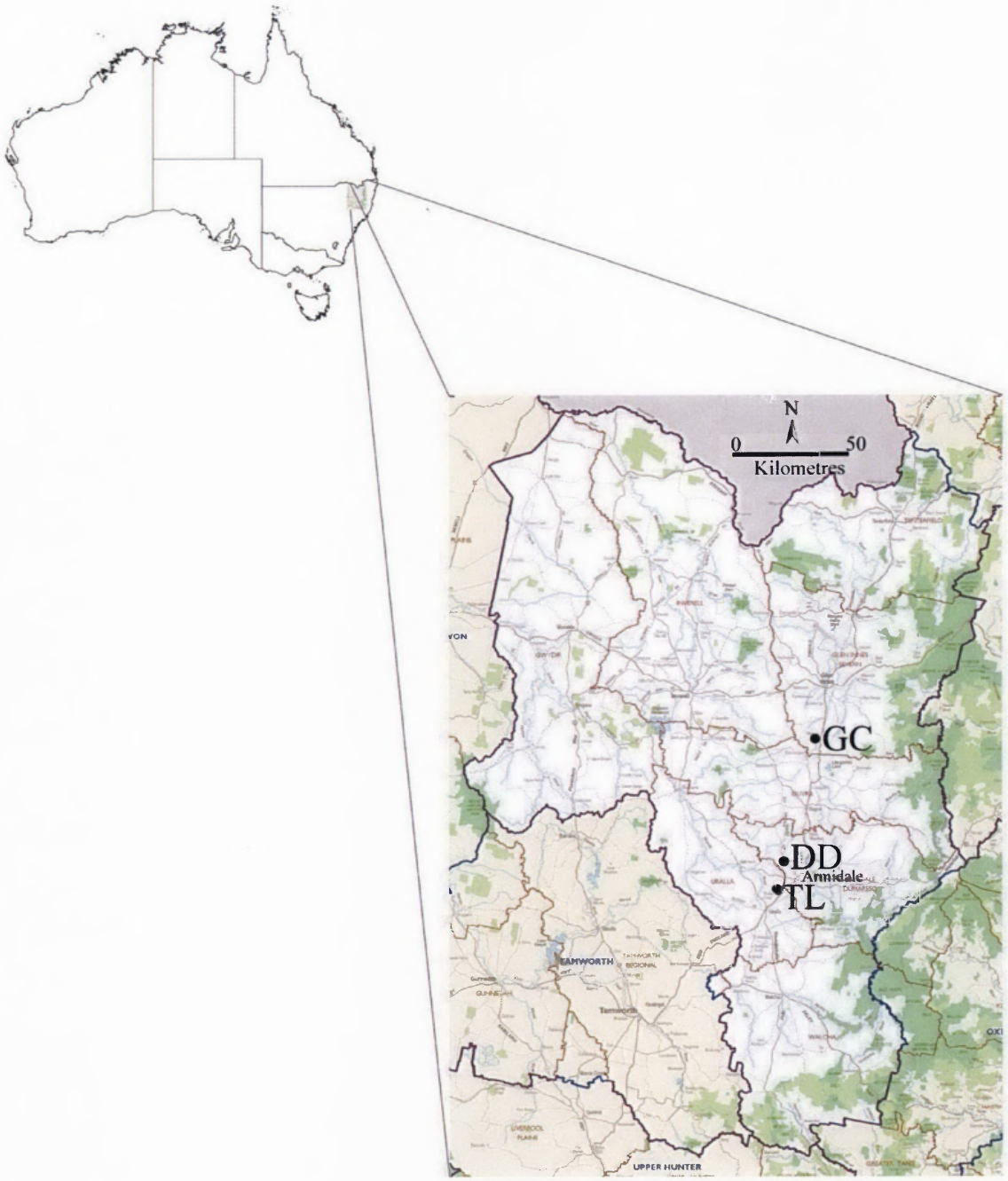

Figure 2.2. Location of study sites of the distylous *Nymphoides montana* in the Northern Tablelands, NSW, Australia. The Dumaresq Dam (DD) population is in a permanent man-made water-body, whereas the Thomas Lagoon (TL) and Glencoe (GC) populations are both naturally occurring and subject to partial flooding with seasonal rainfall. Source: www.aec.gov.au

Figure 2.3. Floral visitors, A) hoverfly, order Diptera; B) butterfly, order Lepidoptera, visiting the S-morph flowers of *Nymphoides montana*.

2.3.3 Population size

To assess the possible effects of population size and density on the reproductive success of the floral morphs, mean flower and plant density were estimated for each of the three populations (DD, TL and GC) by dividing the number of flowers and putative plants (3 m apart) by the area of linear transects, respectively. Transects were 15 m long and 2 m wide.

To assess population size, each population was assumed to be the shape of a circle. The area of the wetland containing *Nymphoides* was calculated as follows (see

Figure 2.4):

a) The circumference of the wetland (outer circle) was measured using 'measurement function' of GoogleEarth, and then, the diameter, radius and area of the wetland were calculated.

b) The width of the plant population (*pw*) was measured, since plants only grow in shallow water at the edge of the wetland.

c) Two *pw* values were subtracted from the diameter of the wetland to calculate the diameter, radius and area of the wetland where plants do not grow (inner circle).

d) The area of *Nymphoides* habitat (population area) was calculated by subtracting the area of the inner circle from the area of the outer circle.

An estimate of overall population size was obtained by multiplying the plant density by the population area. Standard errors (SE) for population size were calculated by multiplying SE for the plant density by the population area, assuming that value is a constant.

Figure 2.4. Aerial photograph of the Glencoe (GC) population showing parameters used to estimate area to calculate population size; pw is the width of plant population. Source: GoogleEarth 6 September 2007

2.3.4 *Morph ratio*

Morph ratio was estimated in March 2005 and in March 2007 by counting flowering plants along the linear transects. The number of transects varied between 15 and 44, depending on the size of the population and the density of plants. It is difficult to identify individual plants in the field because of massive clonal propagation. Two methods, therefore, were used to assess flower morph ratio and putative plant morph ratio in two populations, DD and TL, in 2005. Flower morph ratio was estimated by scoring every flower along the respective transects. Plant morph ratio was estimated by scoring only flowers that were at least 3 m apart, assuming that these represented different plants. Results indicate that flower and plant morph ratios were similar (Table 2.2). The third population (GC) was scored for plant morph ratio only. In 2007, all plants in the TL population were affected by drought and failed to flower. Plant morph ratio, therefore, was assessed in only two populations, DD and GC. Plant morph ratio in each population and heterogeneity among the populations were tested against the expected equilibrium 1:1 ratio typical for distylous species, using the replicated goodness-of-fit test or *G*-test (Sokal and Rohlf 1995).

2.3.5 *Floral measurements*

To examine morph-specific variation in floral traits associated with distyly, one flower from each of 15–20 plants, each at least 3 m apart, per morph in each of the three populations, DD, TL and GC, was randomly collected; this minimised the likelihood of selecting ramets. Flowers were preserved in 70% ethanol until measured. Preserved flowers were slit longitudinally and the base of the superior ovary was considered as the baseline for the height measurements. Measurements were made using a Nikon digital sight DS-L1 attached to a MACROZOOM 1:5 WILD HEERBRUGG dissecting microscope. Most traits were coded using a three-letter code with the first letter indicating the whorl (C: corolla, S: stamen and P: pistil). The measurements were: corolla tube length (CTL), anther height (SAH), anther length (SAL), filament length (SFL), stigma height (PSH), stigma length (PSL) and stigma width (PSW) (Figure 2.5). Stigma–anther separation (SAS) was calculated by subtracting anther height from stigma height for the L-morphs and stigma height from anther height for the S-morphs. Stamen insertion height (SIH) was calculated by subtracting anther length from anther height. Style height (PSY) was calculated by subtracting stigma length from stigma height.

The traits related to flower size and pollinator attraction were measured on 15–20 flowers per morph in each of the two populations, DD and TL. Fresh flowers were used for the measurements to avoid miscalculations due to shrivelled and softened petals. Corolla tube width (CTW) and corolla diameter (CD) were measured to the nearest 0.01 mm using a digital calliper. Corolla lobe length (CLL) was calculated as: (CD − CTW)/2.

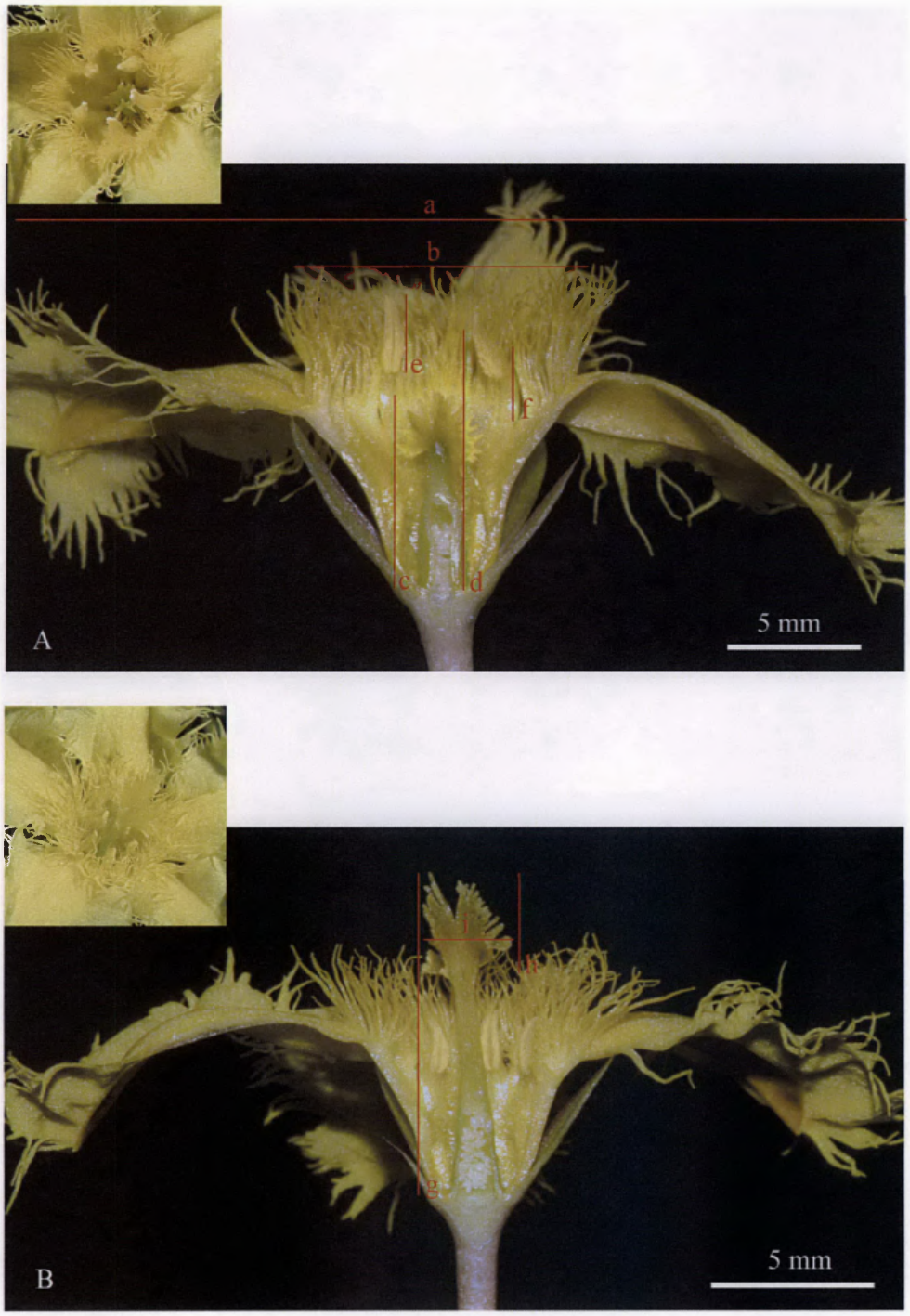

Figure 2.5. Cross-sections of A) the S-morph and B) the L-morph flowers of distylous *Nymphoides montana* from the Dumaresq Dam (DD) population. Letters correspond to the following measurements: a) corolla diameter, b) corolla tube width, c) corolla tube length, d) anther height, e) anther length, f) filament length, g) stigma height, h) stigma length, and i) stigma width.

MINITAB® (ver. 13) was used for all the multivariate and univariate analyses. For the first 10 floral measurements, a multivariate analysis of variance (MANOVA) was used to determine the effects of morph, population and their interaction. Subsequent multivariate analyses involved Principal Component Analysis (PCA) and Discriminant Function Analysis (DFA). In the multivariate analyses, individual data points, rather than population means, were used, since all the floral traits, except traits related to flower size and pollinator attraction, were measured on a single flower from each of 15–20 different plants per morph per population. Principal Component Analysis was used to understand the structure of the data without making *a priori* assumptions about the morphs and populations and to display the data in reduced dimensional space. A covariance matrix was used to extract eigenvalues. Discriminant Function Analysis identified the principle traits that distinguished the morphs.

Floral traits were compared with two-way analyses of variance (ANOVAs), with floral morph and population as fixed and random factors, respectively. When the morph × population interaction was not significant, the interaction was pooled with the error term. Populations with a significant interaction were analysed separately. Here and elsewhere, normality and homogeneity of variances were checked using the Ryan-Joiner test and Levene's test, respectively. Where necessary data, including stigma width, filament length and anther length, were $\log_{10}$ transformed to satisfy assumptions of ANOVA.

2.3.5.1 Phenotypic correlations

The reciprocal arrangement of sex-organ heights between heterostylous morphs is a well-known example of floral design adapted for precision in pollen transfer (see introduction). If an intermorph (plant-to-plant) pollen movement by pollinators is required to successfully set seed, then floral traits involved in efficient pollen transfer from anthers to pollinators and to stigma should increase in integration in floral morphs. If, however, pollinators are not required for seed set, relaxed pollinator-mediated selection should reduce the integration of traits that permit pollen donation and receipt; this likely depends on the extent to which genetic linkage and developmental relationships are strong among floral traits (Conner 2002; Anderson and Busch 2006). Floral integration and its possible role in the evolution of the S-morphs and the L-morphs were assessed using Pearson product moment correlations, which were calculated between 10 floral traits (Table 2.6). Data were pooled across the three populations, DD, TL and GC, to display the phenotypic

correlation matrix, because the variation among the populations was less than the variation between the two morphs. Significance levels for multiple comparisons were adjusted using a sequential Bonferroni test calculated by the Dunn-Šidák method to maintain a specified experimental error rate (α) of 0.05 (Sokal and Rohlf 1995). The number of significant correlations for the correlation matrices of the S-morphs and the L-morphs were compared using a *G*-test.

2.3.5.2 Sex-organ reciprocity

The degree of sex-organ reciprocity was assessed to confirm distyly in *Nymphoides montana* (Thompson *et al.* 1998; Massinga *et al.* 2005). This ratio was calculated for long-level sex organs as:

$$R = (A_{\text{S-morph}} - S_{\text{L-morph}})/(A_{\text{S-morph}} + S_{\text{L-morph}})$$

and for short-level sex organs as:

$$R = (A_{\text{L-morph}} - S_{\text{S-morph}})/(A_{\text{L-morph}} + S_{\text{S-morph}})$$

where A is the anther height of each morph and S is the stigma height of the alternative morph. Standard errors were based on 1000 bootstrap samples, using each individual flower as the unit of re-sampling. To test the null hypothesis of perfect reciprocity ($R = 0$), the distribution of 1000 bootstraps values were examined by sampling with replacement from the original dataset (Eckert and Barrett 1994a; Ramsey *et al.* 2006). A one-tailed test of a given parameter is considered to be either significantly less than or greater than the test value if 100% ($1 - \alpha$) of bootstrap values are either less than or greater than the test value, respectively.

2.3.6 Pollen grain size

To examine dimorphism in pollen grain size between the two morphs, pollen from two flowers from each of 10 randomly chosen plants, each at least 3 m apart, per morph in each of two populations, DD and TL, were collected. Pollen grains were prepared semi-permanently on microscope slides (Beattie 1971). The height and the base of 15 triangular pollen grains on each flower were measured to calculate the area of each pollen grain (Figure 2.6). A total of 1200 pollen grains were measured. The measurements were taken on a Nikon digital sight DS-L1 attached to a light microscope. Pollen grain size was

compared using a two-way ANOVA with floral morph and population as fixed and random factors, respectively. In the preliminary analyses, the population × morph interaction was significant and populations were analysed separately ($F_{1,36} = 11.30$, $P = 0.002$).

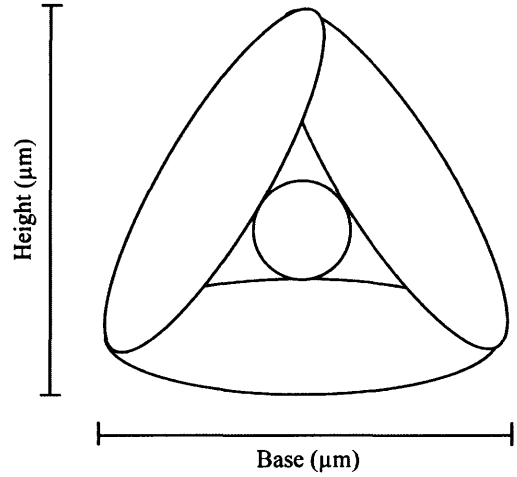

Figure 2.6. Diagram showing how the height and base length of each pollen grain was measured.

2.3.7 Pollen grain number

To examine dimorphism in pollen grain number, the number of pollen grains produced in all five anthers of one flower from each of 15 plants, each at least 3 m apart, per morph in each of two populations, DD and TL, was quantified. Sixty flowers altogether were dissected for the pollen counts. Because the anthers dehisce before the flower opens, each unopened flower was carefully dissected with fine forceps. After the petals and sepals were removed, all five dehisced anthers with the pistil attached to the floral tube were removed and placed in a vial. No visible pollen was lost even though the anthers were dehisced. The anthers were suspended in 400 μl of a solution containing the pollen dye aniline blue. The solution was prepared following Kearns and Inouye (1993). The vial contents were centrifuged for 30 seconds at 1000 rpm in a bench-top centrifuge (Biofuge, Heraeus instruments) and mixed with a vortex mixer (Ratek instruments) prior to counting. All the pollen grains were counted in four replicates of a known volume of the suspension using two haemocytometers. The mean number of pollen grains per flower was calculated by multiplying the mean number of pollen grains by the appropriate dilution factor. To compare pollen grain numbers, a two-way ANOVA was performed with floral morph and

population as fixed and random factors, respectively. The non-significant population × morph interaction was pooled with the error term ($F_{1,56} = 0.76$, $P = 0.388$).

2.3.8 Ovule number

The number of ovules per flower was counted using 10 mature fruit per morph in each of two populations, DD and TL. Ovule number was estimated by adding together the counted number of unfertilised ovules, aborted seeds and mature seeds. Aborted seeds are readily recognisable, being shrivelled with soft brownish seed coats and smaller than mature seeds. To compare ovule number, a two-way ANOVA was used with floral morph and population as fixed and random factors, respectively. The non-significant population × morph interaction was pooled with the error term ($F_{1,36} = 0.41$, $P = 0.526$).

2.3.9 Pollen:ovule ratio

Pollen:ovule ratios provide a conservative estimate of a breeding system (Cruden 1977) and were determined for each morph from two populations, DD and TL. The numbers of pollen grains and ovules were counted on different individuals. Mean pollen and ovule numbers were used to calculate the pollen:ovule ratios. A bootstrapping procedure was performed whereby pollen grain number and ovule number were randomly re-sampled with replacement from the original data to calculate standard errors.

2.3.10 Pollen and stigma morphology

Variation in pollen grain sculpture and stigmatic papilla size and shape associated with the two morphs, was examined using scanning electron microscopy (SEM). Two or three samples were dissected from mature flowers from each of two individual plants, each at least 3 m apart, per morph per population (DD and TL). The samples were fixed in FPA (Formalin:Propionic acid:Ethanol = 5%:5%:90%) then stored in 70% ethanol. The fixed materials were dehydrated in an alcohol series of 70% ethanol (5 min), then 80, 90, 95 and 100% ethanol (10 min each). Finally the dehydrated specimens were critical point dried and covered in gold. The samples were viewed under various magnifications with a JEOL JSM-5800LV (Tokyo, Japan) scanning electron microscope.

2.3.11 Incompatibility systems

During February and March 2005, 60 plants (20 plants/morph/population) were collected randomly from two populations, DD and TL. Plants of the same morph type were

collected at least 3 m apart to avoid repeated sampling of plants resulting from clonal propagation. The plants were placed in 10-cm pots with a medium to heavy soil mixture (loam:sand:clay = 2:1:1) and transferred to a pollinator-free glasshouse at 10–28°C and 90–92 % humidity (Botany, UNE). Percent humidity was assessed using a hygrometer (Hygrometer, NSW, Australia). Pots were arranged in plastic containers and filled with rain water so that the water was at soil level (Figure 2.7 A). Plants were fertilized with Hysol® a hydroponic nutrient solution, according to the manufacturer's instructions. Additional light (Wotan Power Star HQI-R 250 W/NDL, Wotan Lamps Ltd., London) was supplied for a period of 6 h per day during the cooler seasons.

Self- and intramorph incompatibility were assessed using controlled pollinations on 15 plants of each morph from the DD population and 19 plants of each morph from the TL population. For each plant, 7–9 flowers were allocated to the following pollination treatments: a) self-pollination – stigmas received pollen from the same flower, b) intramorph pollination (illegitimate cross) – stigmas received cross-pollen from another plant of the same morph type and c) intermorph pollination (legitimate cross) – stigmas received cross-pollen from another plant of the opposite morph type. There were 2–3 replicate flowers on each plant. Treated flowers were labelled with water-proof sticky tape (Figure 2.7 B). Mature fruits were scored and harvested 3–4 weeks later.

Percent fruit set was calculated by scoring the number of mature fruits containing at least one seed, and the result was analysed using a logistic model and analysis of deviance with a binomial error structure and a logit-link function to examine the effects of population, morph and pollination treatment and all two-way interactions. Analyses were conducted using the statistical package GLMStat (ver. 6, Beath 2000).

Seed set was determined by counting the number of mature seeds in each fruit using a LEICA MZ6 dissecting microscope. A split-plot analysis of variance (ANOVA) was used to test the effects of population, plant, morph, and pollination treatment on the number of mature seeds per fruit. Floral morph and pollination treatment were considered fixed factors. Population and plant nested within population and morph were considered random factors. In the preliminary analyses, the population × morph × pollination treatment interaction term was not significant and was excluded from the final model ($F_{2,97} = 0.23$, $P = 0.796$). Normality and homogeneity of variance of the seed set data were greatly improved using Taylor's power law transformation (Fry 1993). For tests that required a

synthetic denominator mean square, the denominator degree of freedom was calculated using Satterthwaite's test. Self-incompatibility indices (SII) were calculated for the S-morphs and the L-morphs using seed set and fruit set from self- and cross-pollinations following Lloyd and Schoen (1992).

Figure 2.7. Photographs of the distylous *Nymphoides montana* showing A) glasshouse plants and B) a mature fruit on the left and a young fruit on the right.

2.3.12 Autonomous self-fertilisation

Fruit set and seed set in the absence of pollinators (autonomous self-fertilisation) were assessed on 30–40 flowers per morph in each of two populations, DD and TL, under glasshouse conditions. Flowers were left untouched and not pollinated. Percent autonomous fruit set was estimated by calculating the proportion of flowers developing to mature fruits. Percent fruit set was analysed using logistic model and analysis of deviance with a binomial error structure and a logit-link function to examine the effects of population and morph (Crawley 1993). The statistical package GLMStat (ver. 6, Beath 2000) was used for the analyses. Autonomous seed set was estimated by counting the number of mature seeds per fruit. Since an average of one seed per L-morph fruit was produced in both study populations, seed set of the S-morphs was compared between the two populations using a 2-sample *t*-test assuming equal variances. Autonomous self-fertilisation index (AFI) was calculated for the S-morphs using seed set and fruit set from auto-and cross-pollinations following Lloyd and Schoen (1992).

2.3.13 Open pollinations

Open-pollinated fruit set and seed set were estimated in March 2005 and March 2007 to assess reproductive success of the floral morphs under natural pollinations. In March 2005, the open pollination experiment was conducted in two populations, DD and TL. In March 2007, however, the experiment was carried out only in the DD population. No data were available from the drought-affected TL population. Total numbers of open-pollinated flowers and mature fruits per morph per population per year are given in Table 2.9.

Fruit set was assessed by labelling open-pollinated flowers with coloured flag tape to differentiate morph types in the fields. Mature fruits were scored 2–3 weeks later. The proportion of flowers forming to mature fruits was counted to calculate percent fruit set. An analysis of deviance was used to compare percent fruit set between the morphs and the populations as described in section 2.3.12.

Seed set was assessed by dissecting mature fruits of each morph in each population under a LEICA MZ6 dissecting microscope. Percent seed set was calculated from the proportion of ovules forming to mature seeds. Percent seed set was compared using, a two-way ANOVA with floral morph and population as fixed and random factors, respectively. In the preliminary analyses, the population × morph interaction was marginally significant,

and the two populations were analysed separately ($F_{1,139}$ = 2.78, P = 0.098). A one-way ANOVA was used to compare percent seeds set in the DD population in 2007.

The percent seed set between 2005 and 2007 in the DD population was compared using a two-way ANOVA with floral morph and year as fixed and random factors, respectively. In the preliminary analyses, the year × morph interaction was significant and the two morphs were analysed separately ($F_{1,125}$ = 10.24, P = 0.002).

2.4 Results

2.4.1 Population size

Populations of *Nymphoides montana* varied in size and density (Table 2.1). In the TL population with low flowering plant density, each flowering ramet was a representative of a single plant, whereas the DD population was more dense with each plant producing a few ramets (Table 2.1).

Table 2.1. Population densities and sizes of the distylous *Nymphoides montana* in the Thomas Lagoon (TL), Dumaresq Dam (DD) and Glencoe (GC) populations. Values for flower and plant densities are means ± SE. See section 2.3.3 for methods to calculate standard errors for population size.

Population	Density (m^{-2})		Population area (m^2)	Population size
	Flower	Plant		
TL	0.05 ± 0.01	0.05 ± 0.01	3544 ± 394	142 ± 35
DD	0.67 ± 0.28	0.67 ± 0.28	13718 ± 5733	2,469 ± 686
GC	—	—	285480 ± 31720	1,022,018 ± 105,628

2.4.2 Morph ratio

In 2005, the frequency of the L-morph and the S-morph plants in each population did not differ from a 1:1 ratio, and there was no significant heterogeneity in floral morph frequencies among the three populations (Table 2.2). However, the L-morphs significantly outnumbered the S-morphs in the DD population in 2007, whereas in the GC population the ratio between the morphs was close to 1 (Table 2.2). There was no significant heterogeneity in the morph frequencies between the DD and the GC populations in 2007 (Table 2.2).

Table 2.2. Morph frequencies of the S-morphs and the L-morphs of *Nymphoides montana* in the Thomas Lagoon (TL), Dumaresq Dam (DD) and Glencoe (GC) populations in 2005 and 2007. A 1:1 morph ratio was observed in all the populations in 2005. The DD population, however, became L-biased in 2007. No data were available from the TL population in 2007. Superscripts denote: * $P<0.05$ and ** $P<0.01$ in a G-test for inequality of frequencies.

Population	**2005**						**2007**			
	Morph ratio						**Morph ratio**			
	Flower		**Plant**				**Plant**			
	S-morph	**L-morph**	**S-morph**	**L-morph**	**df**	***G***	**S-morph**	**L-morph**	**df**	***G***
TL	0.47	0.53	0.48	0.52	1	0.24	—	—	—	—
DD	0.48	0.52	0.45	0.55	1	0.82	0.39	0.61	1	4.71^{**}
GC	—	—	0.48	0.52	1	0.27	0.47	0.53	1	0.24
			Pooled		1	1.08	Pooled		1	4.09^{**}
			Heterogeneity		2	0.92	Heterogeneity		1	0.87
			Total		3	2.00	Total		2	4.96^{*}

2.4.3 Between-morph and population variations in floral traits

Nymphoides montana has two floral morphs that differ in the position of the anthers and the stigmas (Figure 2.1). In the flowers of the L-morph, the stigma is exserted and the stamens surround the throat of the corolla tube. Flowers of the S-morph plants have a short stigma located above the midpoint of the corolla tube, whereas the stamens are noticeably exserted and lean down toward the centre of the flower.

The MANOVA showed a significant effect of morph (Wilk's $\lambda = 0.13$; $F_{9,76} = 626.52$; $P < 0.001$), a significant effect of population (Wilk's $\lambda = 0.09$; $F_{18,152} = 19.83$; $P < 0.001$) and a significant population × morph interaction (Wilk's $\lambda = 0.14$; $F_{18,152} = 13.82$; $P < 0.001$) on floral measurements.

The loadings of the floral traits of the PCA are given in Table 2.3. The first three principal components explained ≥ 96% of the variation in the traits (Table 2.3). The L-morphs and the S-morphs formed two distinct, non-overlapping groups along the PC1 axis (Figure 2.8). For the PC1 scores, stigma height had a strong loading, while other traits contributed little (Table 2.3). For the PC2 scores, anther height and to a lesser extent stamen insertion height had strong loadings (Table 2.3). The PCA also shows that the two morphs of the TL population are located closely along PC1 and similar along PC2, indicating the stigma height, anther height and stamen insertion height of these morphs are the parameters with least variability in the data set. In the DFA, cross validation verified this result and 90% of the total variation among the individuals was correctly classified. Correct classifications to the morph type were 100%.

Table 2.3. Loading of traits on the first three scores in the Principal Component Analysis. Eigenvalues and percent total variance are given in parentheses and brackets, respectively. Character loadings of an absolute value > 0.50 are given in bold. PC1, PC2 and PC3 are defined as the first, second and third principle components, respectively.

Traits	PC1 (12.24) [80.6]	PC2 (1.89) [12.4]	PC3 (0.45) [2.9]
Stigma height	**−0.66**	−0.24	0.04
Stigma width	−0.19	−0.10	0.06
Stigma length	−0.28	−0.07	−0.43
Style length	−0.38	−0.17	0.47
Anther height	0.31	**−0.59**	−0.25
Filament length	0.20	−0.18	0.00
Anther length	0.05	−0.09	**−0.51**
Stamen insertion height	0.25	**−0.50**	0.26
Stigma–anther separation	−0.33	−0.35	−0.33
Corolla tube width	0.08	−0.38	0.30

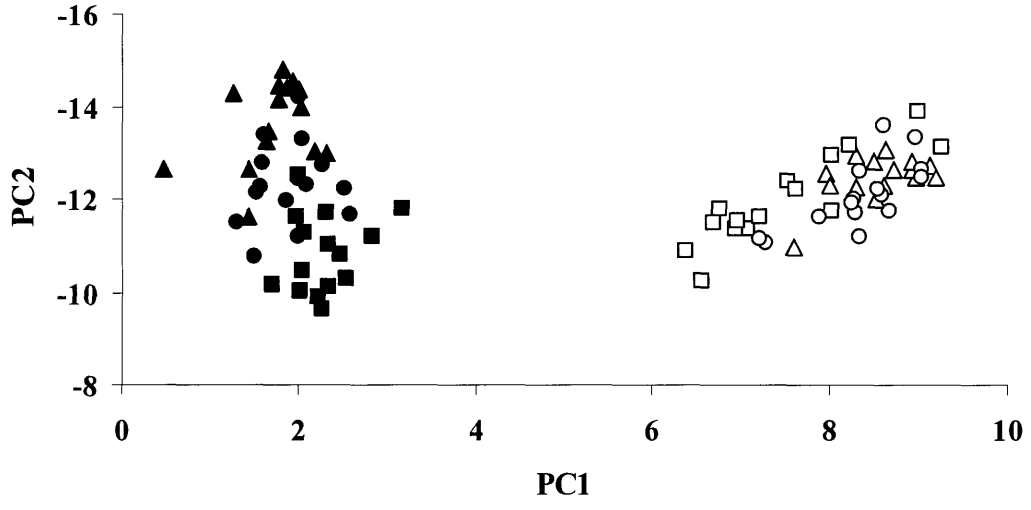

Figure 2.8. Plot of the first (PC1) and second (PC2) principal component scores for the S-morphs (left, filled symbols) and the L-morphs (right, open symbols) of *Nymphoides montana* from the Dumaresq Dam (DD; ▲Δ), Thomas Lagoon (TL; ■□) and Glencoe (GC; ○●) populations. The 10 floral traits used in the analysis are described in Table 2.3. PC1 and PC2 explained 80.6% and 12.4% of the variation among the individuals, respectively.

The mean values and the results of the ANOVAs on all the floral traits studies are given in Table 2.4 and Table 2.5, respectively. In all three populations, female traits of the L-morphs, including stigma height, stigma width, stigma length and style length, were significantly larger than those of the S-morphs (one-way ANOVAs; PSL: all $F_{1,28} \geq 135.80$, all $P < 0.001$). In contrast, male traits of the S-morphs, including anther height, anther length, filament length and stamen insertion height, were significantly larger than those of L-morphs (one-way ANOVAs; SAH: all $F_{1,28} \geq 38.49$, all $P < 0.001$; SFL: all $F_{1,28} \geq 140.87$, all $P < 0.001$; SIH: all $F_{1,28} \geq 23.80$, all $P < 0.001$). The S-morphs showed a significantly reduced stigma–anther separation compared with the L-morphs in all populations (Table 2.5). Variation among the populations was significant for most floral traits (Table 2.5).

Traits related to flower size and pollinator attraction were significantly different between the two morphs. Corolla tube length and corolla tube width of the S-morphs were significantly greater than the L-morphs, although the trend was only marginally significant for the TL population (one-way ANOVAs; CTL: all $F_{1,28} \geq 3.93$, DD and GC $P < 0.001$, TL $P = 0.057$). However, corolla lobe length of the S-morphs was significantly shorter than the L-morphs (one-way ANOVAs; DD: $F_{1,24} = 30.10$, $P < 0.001$ and TL: $F_{1,28} = 28.58$, $P < 0.001$). Corolla diameter of the S-morphs was significantly decreased compared with the L-morphs in the DD population but not in the TL population (one-way ANOVAs; DD: $F_{1,24} = 6.02$, $P < 0.001$; TL: $F_{1,28} = 0.02$, $P = 0.882$).

Table 2.4. Floral traits (means in mm ± S.E.) of the S-morphs and the L-morphs in *Nymphoides montana*. The first 10 traits were measured on a flower from each of 15–20 plants per morph in each of the Dumaresq Dam (DD), Thomas Lagoon (TL) and Glencoe (GC) populations. These traits were used for Principal Component Analysis (PCA) and Discriminate Function Analysis (DFA). Traits 11–13 were measured on 13–15 fresh flowers per morph in each of two populations, DD and TL. Since fresh flowers were not collected from the GC population, the traits related to flower size and pollinator attraction could not be measured.

No.	Traits	Populations					
		DD		TL		GC	
		S-morph	L-morph	S-morph	L-morph	S-morph	L-morph
1	Stigma height	6.17 ± 0.14	10.71 ± 0.12	5.55 ± 0.11	9.66 ± 0.24	5.83 ± 0.11	10.43 ± 0.12
2	Stigma width	2.39 ± 0.09	3.71 ± 0.11	2.00 ± 0.04	3.29 ± 0.10	2.04 ± 0.05	3.25 ± 0.09
3	Stigma length	1.81 ± 0.07	3.81 ± 0.07	1.54 ± 0.05	2.83 ± 0.10	1.72 ± 0.06	3.89 ± 0.12
4	Style length	4.37 ± 0.13	6.81 ± 0.10	4.01 ± 0.09	6.83 ± 0.22	4.11 ± 0.09	6.55 ± 0.17
5	Anther height	8.99 ± 0.16	5.92 ± 0.07	6.88 ± 0.16	5.74 ± 0.10	8.32 ± 0.14	5.90 ± 0.11
6	Filament length	2.33 ± 0.07	0.63 ± 0.02	1.67 ± 0.06	0.65 ± 0.04	1.94 ± 0.06	0.44 ± 0.02
7	Anther length	2.07 ± 0.15	1.74 ± 0.04	1.78 ± 0.08	1.37 ± 0.03	2.59 ± 0.03	2.05 ± 0.04
8	Stamen insertion height	6.92 ± 0.16	4.18 ± 0.07	5.11 ± 0.12	4.37 ± 0.10	5.74 ± 0.15	3.85 ± 0.08
9	Stigma–anther separation	2.81 ± 0.13	4.79 ± 0.11	1.33 ± 0.11	3.92 ± 0.17	2.49 ± 0.11	4.56 ± 0.12
10	Corolla tube length	8.35 ± 0.10	6.86 ± 0.07	6.77 ± 0.16	6.16 ± 0.11	7.11 ± 0.10	6.60 ± 0.08
11	Corolla tube width	7.84 ± 0.22	5.23 ± 0.11	7.34 ± 0.23	4.79 ± 0.11	—	—
12	Corolla lobe length	10.73 ± 0.26	13.27 ± 0.35	10.80 ± 0.11	12.12 ± 0.22	—	—
13	Corolla diameter	29.29 ± 0.62	31.77 ± 0.11	28.94 ± 0.34	29.03 ± 0.50	—	—

Table 2.5. Results of two-way ANOVAs examining 13 floral traits of *Nymphoides montana*. Analyses correspond to means (± SE) given in Table 2.4. A dash (—) indicates a non-insignificant population × morph interaction ($P > 0.09$) which was pooled with the error term for the final analysis. When the interaction was significant ($P < 0.09$) populations were analysed separately (see the text). Superscripts denote: NS > 0.09, † $0.05 < P < 0.09$, * $P < 0.05$, ** $P < 0.01$, *** $P < 0.001$.

No.	Traits	Population	Morph	Population × morph
1	Stigma height	15.00^{***}	1232.01^{***}	—
2	Stigma width	16.16^{***}	386.28^{***}	—
3	Stigma length	41.38^{***}	44.33^{*}	17.26^{***}
4	Style length	1.78^{NS}	496.06^{***}	—
5	Anther height	43.29^{***}	$15.24^{\dagger}$	30.26^{***}
6	Filament length	17.31^{***}	64.07^{*}	17.12^{***}
7	Anther length	55.73^{***}	46.32^{***}	—
8	Stamen insertion height	30.55^{***}	$9.44^{\dagger}$	37.65^{***}
9	Stigma–anther separation	46.53^{***}	127.86^{**}	3.54^{*}
10	Corolla tube length	28.15^{***}	0.98^{NS}	37.64^{***}
11	Corolla tube width	7.43^{**}	223.80^{***}	—
12	Corolla lobe length	0.79^{NS}	10.08^{NS}	5.81^{*}
13	Corolla diameter	1.69^{NS}	1.16^{NS}	4.39^{*}

Degrees of freedom for the first 10 traits: 2,84 for population, 1,2 for morph, and 2,84 for the population × morph interaction. Degrees of freedom when the non-significant interaction ($P > 0.09$) was pooled with the error: 2,86 for population and 1,86 for morph.

Degrees of freedom for the last three traits: 1,52 for population, 1,1 for morph, and 1,52 for the population × morph interaction. Degrees of freedom when the non-significant interaction ($P > 0.09$) was pooled with the error: 1,53 for both population and morph.

2.4.3.1 Phenotypic correlations

The phenotypic correlations showed that corolla tube length was significantly correlated with stigma height, anther height and stigma–anther separation in the S-morphs but not the L-morphs (Table 2.6). Male traits, including anther height, filament length and stamen insertion height were significantly correlated with stigma–anther separation only in the S-morphs (Table 2.6). Female traits, including stigma height, stigma length and style length were significantly correlated with stigma–anther separation only in the L-morphs (Table 2.6). Correlation matrices for the S-morphs showed a significantly higher number of significant correlations compared with correlation matrices for the L-morphs ($\chi^2 = 6.40$, df = 1, $P = 0.011$).

Table 2.6. Pearson correlation coefficients and associated probabilities for floral traits measured on 45 S-morphs and 45 L-morphs from the three populations, DD, TL and GC, of *Nymphoides montana*. Corolla tube length was correlated with the stigma and anther heights as well as stigma–anther separation in the S-morphs, only. Stigma–anther separation was correlated with the male traits of the S-morphs and the female traits of the L-morphs. The significance levels after correction for multiple comparisons with a sequential Bonferroni test are given in bold (Sokal and Rohlf 1995).

	PSH	PSW	PSL	PSY	SAH	SFL	SAL	SIH	SAS
S-morphs									
PSW	0.523								
	<0.001								
PSL	0.603	0.223							
	<0.001	0.141							
PSY	0.878	0.513	0.147						
	<0.001	**<0.001**	0.334						
SAH	0.708	0.489	0.545	0.551					
	<0.001	**0.001**	**<0.001**	**<0.001**					
SFL	0.627	0.449	0.526	0.462	0.785				
	<0.001	**0.002**	**<0.001**	**0.001**	**<0.001**				
SAL	0.245	−0.040	0.443	0.038	0.475	0.178			
	0.105	0.792	**0.002**	0.802	**0.001**	0.241			
SIH	0.670	0.579	0.376	0.605	0.877	0.794	−0.006		
	<0.001	**<0.001**	0.011	**<0.001**	**<0.001**	**<0.001**	0.967		
SAS	0.139	0.377	0.046	0.145	0.635	0.586	−0.194	0.828	
	0.363	0.011	0.763	0.343	**<0.001**	**<0.001**	0.202	**<0.001**	
CTL	0.499	0.493	0.429	0.361	0.730	0.598	0.096	0.777	0.660
	<0.001	**0.001**	0.003	0.015	**<0.001**	**<0.001**	0.532	**<0.001**	**<0.001**
L-morphs									
PSW	0.499								
	<0.001								
PSL	0.616	0.407							
	<0.001	0.006							
PSY	0.652	0.229	−0.196						
	<0.001	0.130	0.196						
SAH	0.659	0.388	0.329	0.504					
	<0.001	0.008	0.027	**<0.001**					
SFL	0.106	0.284	−0.225	0.349	0.281				
	0.487	0.059	0.137	0.019	0.062				
SAL	0.443	0.099	0.672	−0.096	0.379	−0.448			
	0.002	0.518	**<0.001**	0.530	0.010	0.002			
SIH	0.263	0.288	−0.244	0.562	0.641	0.639	−0.467		
	0.081	0.055	0.106	**<0.001**	**<0.001**	**<0.001**	**0.001**		
SAS	0.903	0.416	0.600	0.546	0.272	−0.024	0.350	−0.031	
	<0.001	0.004	**<0.001**	**<0.001**	0.071	0.873	0.019	0.841	
CTL	0.131	0.120	−0.331	0.482	0.373	0.563	−0.482	0.756	−0.045
	0.389	0.433	0.026	**0.001**	0.012	**<0.001**	**0.001**	**<0.001**	0.767

PSH = stigma height, PSW = stigma width, PSL = stigma length, PSY = style length, SAH = anther height, SFL = filament length, SAL = anther length, SAL = anther length, SIH = stamen insertion height, SAS = stigma–anther separation and CTL = corolla tube length.

2.4.3.2 Sex-organ reciprocity

The reciprocity indices based on stigma heights and anther heights of the two morphs are shown in Figure 2.9. There was weak reciprocity between the long-level sex organs, and reciprocity was significantly less than zero (Figure 2.9). This result means the S-morph anthers and the L-morph stigmas were not positioned at equivalent heights because of the reduced stigma–anther separation of the S-morphs in all the populations (Figure 2.10). In contrast, the short-level sex organs showed a perfect reciprocity (Figure 2.9). The L-morph anthers and the S-morph stigmas were positioned at reciprocal heights in all populations (Figure 2.10), and reciprocity did not differ significantly from zero (Figure 2.9).

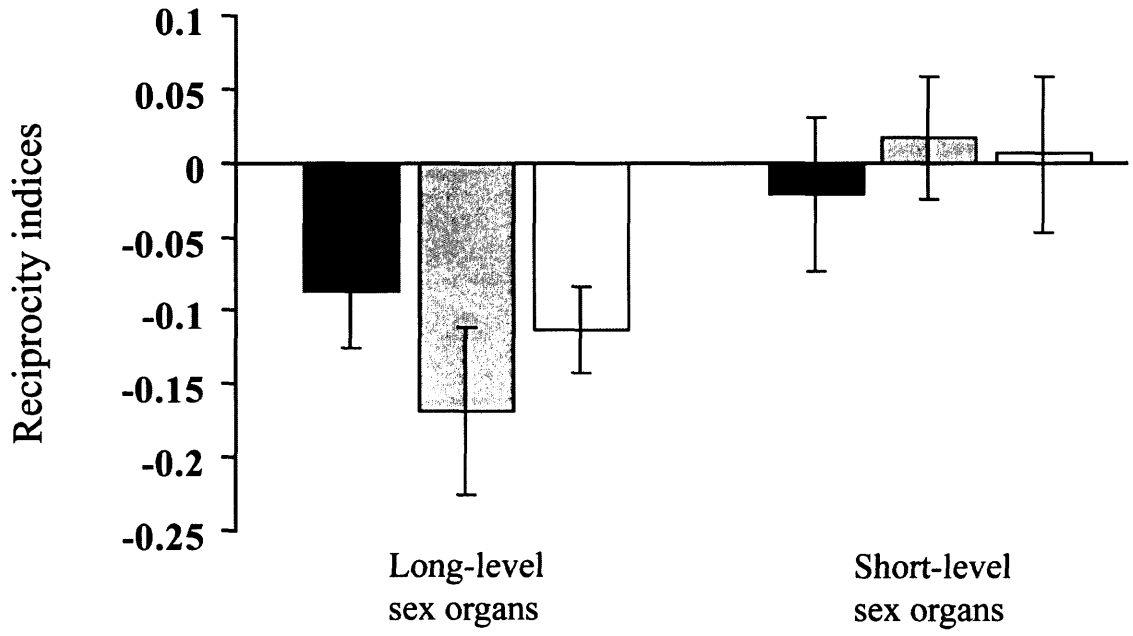

Figure 2.9. Reciprocity indices between long-level sex organs and short-level sex organs of *Nymphoides montana* in the Dumaresq Dam (DD; ■), Thomas Lagoon (TL; ■), and Glencoe (GC; □) populations. Reciprocity between the long-level organs was significantly less than zero (all $P < 0.001$), whereas reciprocity between the short-level organs did not differ from zero (all $P > 0.05$).

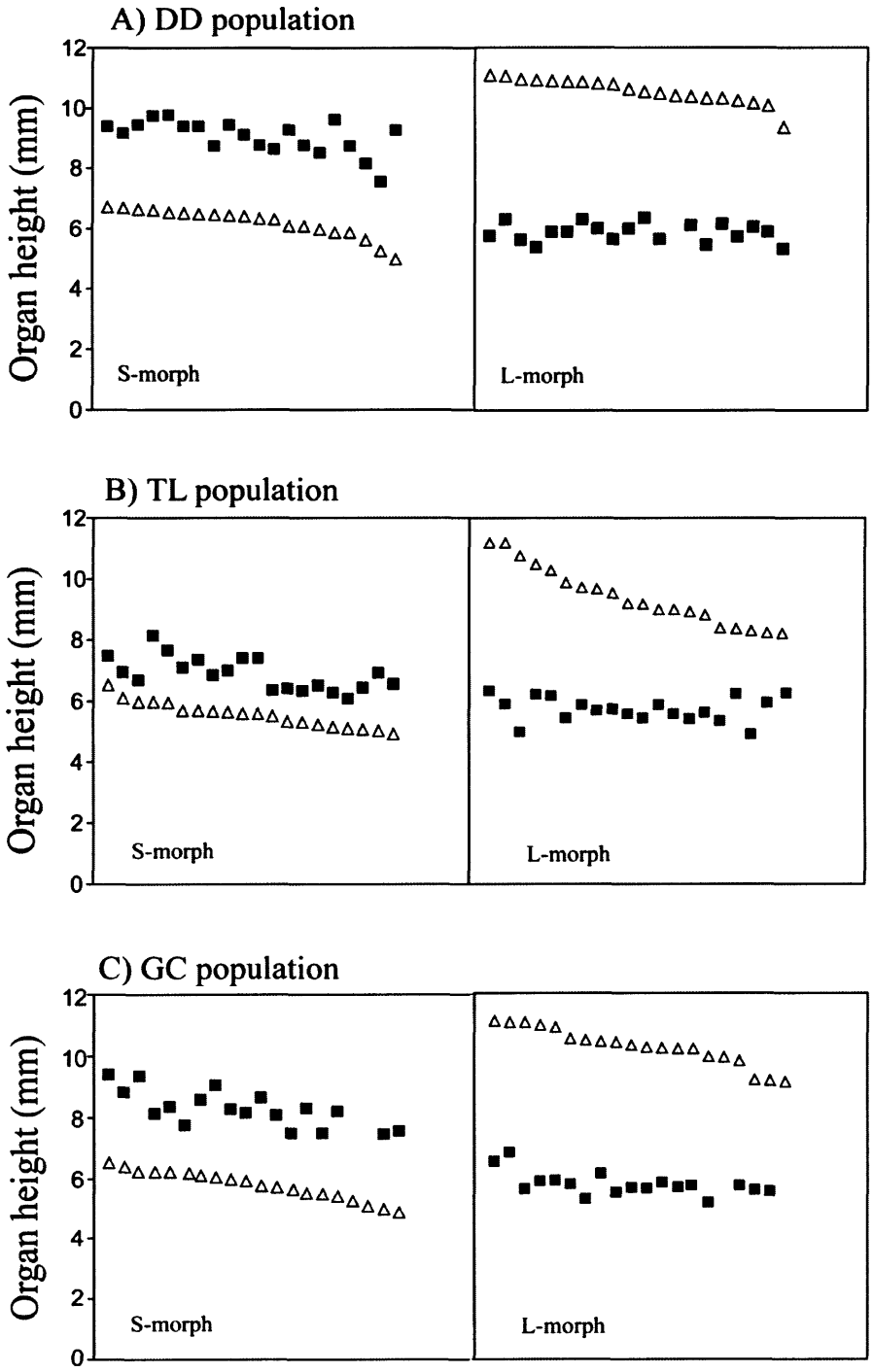

Figure 2.10. Sex-organ heights of *Nymphoides montana* showing the position of the anthers (■) and the stigmas (Δ) in a sample of 20 S-morph flowers and 20 L-morph flowers from each of A) Dumaresq Dam (DD), B) Thomas Lagoon (TL) and C) Glencoe (GC) populations. Flowers are ranked by the stigma height. The short-level stigmas and the short-level anthers are positioned reciprocally, whereas the long-level stigmas and the long-level anthers are not at equivalent heights.

2.4.4 Pollen grain size and number, and ovule number

Pollen grain size differed significantly between the morphs, with the S-morph pollen being 45–55 % larger than the L-morph pollen in the DD and TL populations (Figure 2.11 A, B; one-way ANOVAs; both $F_{1,18} \geq 637.87$, both $P < 0.001$). However, the S-morphs produced significantly less pollen than the L-morphs in both populations (Table 2.7; $F_{1,57} = 27.10$, $P < 0.001$). There was no significant difference between the populations in pollen grain number ($F_{1,57} = 2.68$, $P = 0.107$).

There was no significant difference between the morphs in the number of ovules per flower in the DD and TL populations (Table 2.7; $F_{1,37} = 2.47$, $P = 0.125$). Variation between the populations was not significant ($F_{1,37} = 1.75$, $P = 0.194$). The pollen:ovule ratios were relatively high in both morphs (DD: S-morph = 545.55 ± 130.89, L-morph = 797.39 ± 269.51 and TL: S-morph = 386.28 ± 164.48, L-morph = 706.67 ± 217.05), corresponding to a facultative outcrossing breeding system (Cruden 1977).

Table 2.7. Mean (± SE) pollen grain size and number, and ovule number in the S-morphs and the L-morphs of *Nymphoides montana* from the Dumaresq Dam (DD) and Thomas Lagoon (TL) populations. The S-morphs produced larger and fewer pollen grains than the L-morphs. Ovule number did not differ between the morphs.

Traits	**Populations**			
	DD		**TL**	
	S-morph	**L-morph**	**S-morph**	**L-morph**
Pollen grain size (μm)	388.38 ± 4.81	249.97 ± 2.62	373.42 ± 3.09	257.00±1.79
Pollen grain number	41533 ± 2225	55467 ± 3645	33467 ± 3539	53000 ± 3280
Ovule number	74.03 ± 3.75	66.57 ± 1.67	76.44 ± 4.40	72.77 ± 2.55

2.4.5 Pollen and stigma morphology

At anthesis, the anthers split longitudinally and release pollen grains at the tetrahedral tetrad stage. The pollen grains are triangular and 3-colporate (Figure 2.11 A, B). However, the pollen sculpture between the two morphs differs. The SEM images of pollen grains show that the muri of the S-morph pollen grains have minute granulae over the whole pollen surface (Figure 2.11 C), whereas the muri of the L-morph pollen grains are smooth (Figure 2.11 D).

Stigmas of both morphs are divided into two deltoid ascending lobes (Figure 2.12 A, B). In the S-morphs, each lobe is divided into five crateriform sub-lobes (Figure 2.12 A), whereas in the L-morphs, each lobe is divided into two sub-lobes (Figure 2.12 B). Stigmatic papillae are spread on both the interior and exterior surfaces of the S-morph stigmatic lobes. In the L-morph stigmas, papillae cover the inner and outer marginal areas of finger-like projections of the lobes with the broad deltoid area lacking papillae. The stigmatic papillae vary in shape and size between the two morphs with the spherical S-morph papillae shorter (Figure 2.12 C) than the cylindrical papillae of the L-morphs (Figure 2.12 D).

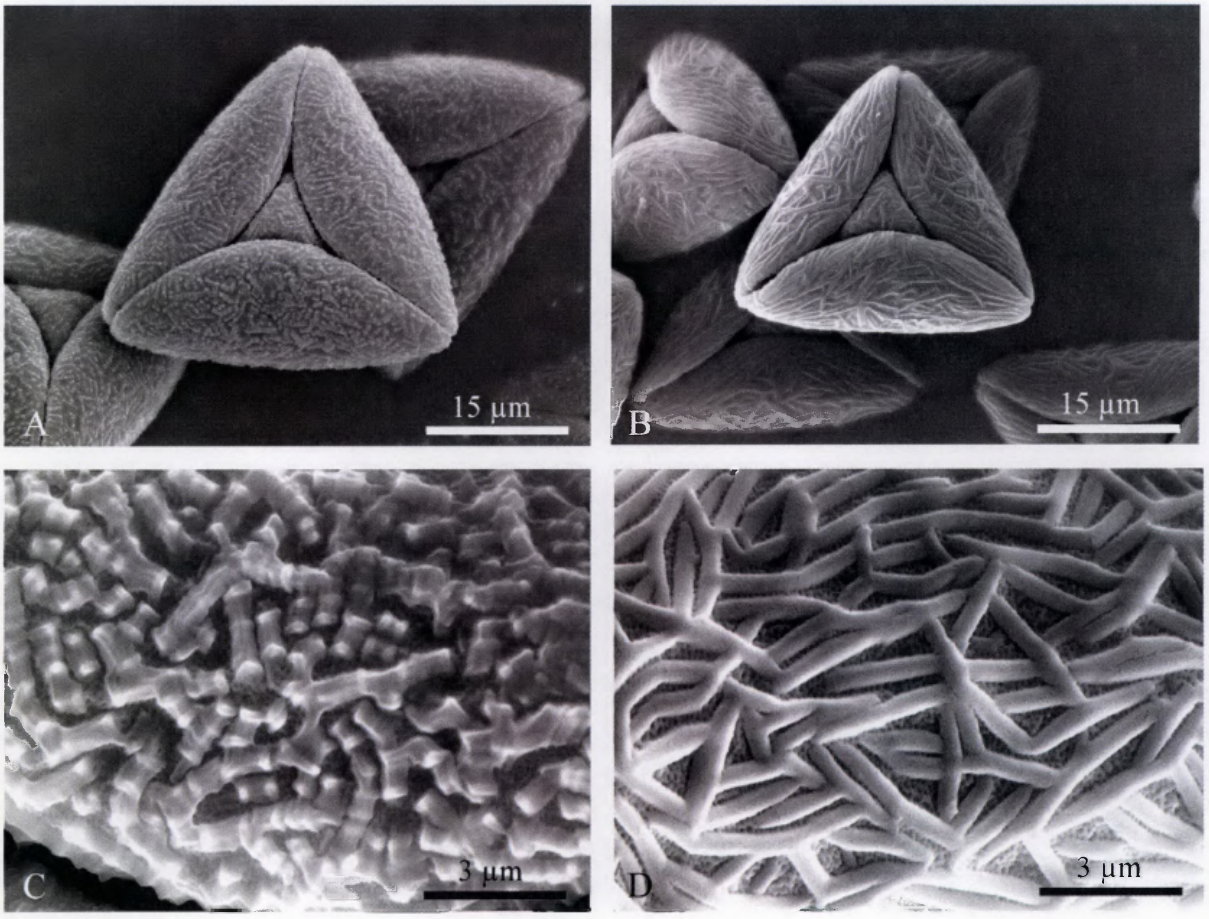

Figure 2.11. SEM micrographs of air-dried pollen grains of the S-morph (A and C) and the L-morph (B and D) of *Nymphoides montana* showing pollen size dimorphism and variations in the pollen exine sculpture. The S-morph pollen is larger (A) with a rough pollen surface (C); the smaller L-morph pollen (B) has a smooth surface (D).

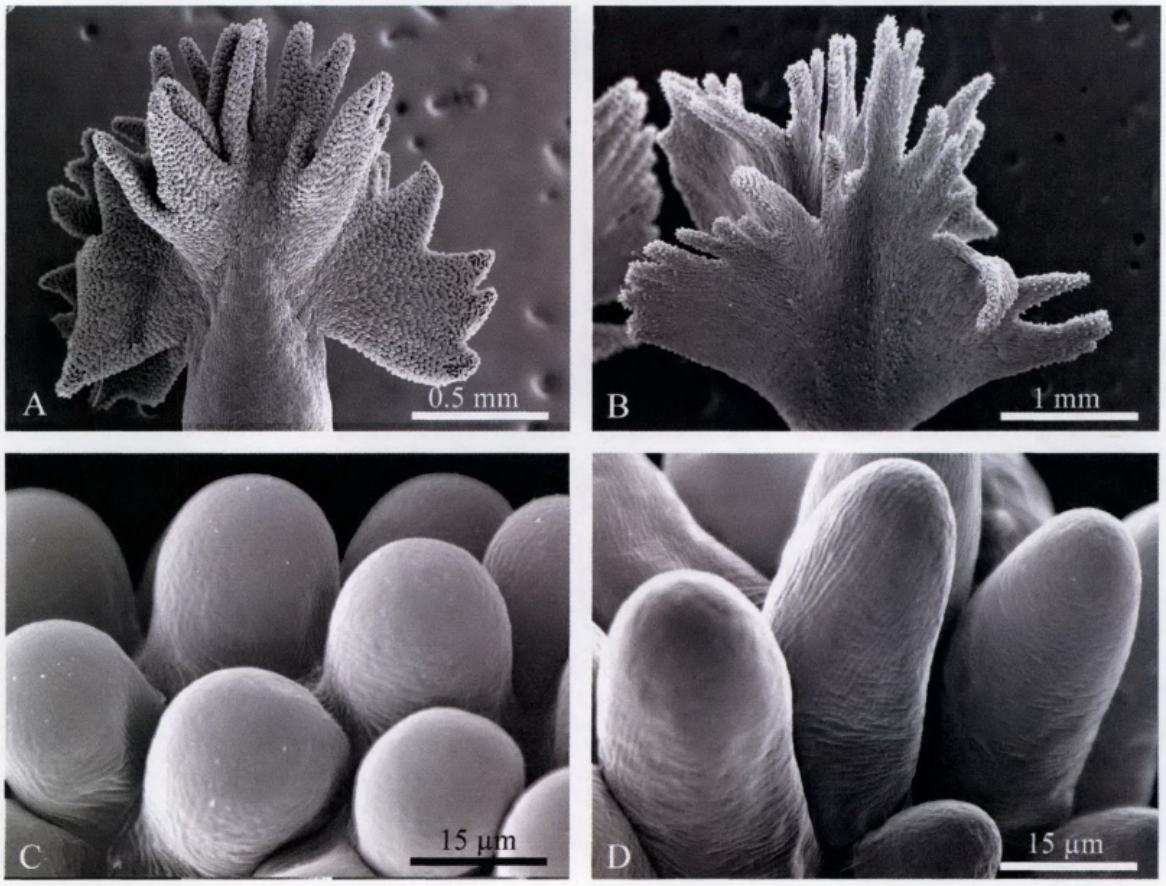

Figure 2.12. SEM micrographs of the S-morph stigma (A and C) and the L-morph stigma (B and D) of *Nymphoides montana* showing dimorphism in stigma size and shape. Stigmas of both morphs are bilobed, the ascending lobes deltoid. The S-morphs have five sub-lobes per lobe (A) and the L-morphs two sub-lobes (B). The S-morph stigmatic papillae are short and spherical (C) and the L-morph stigmatic papillae are long and cylindrical (D).

2.4.6 Incompatibility systems

The results of the analysis of deviance on hand-pollinated fruit set showed that both morphs and pollination treatments differed significantly (morph: $\chi^2 = 54.09$, df = 1, $P < 0.0001$; pollination treatment: $\chi^2 = 150.70$, df = 1, $P < 0.0001$). In both populations, fruit set of the L-morphs following self- and intramorph pollinations was about 40% with the S-morphs about 80% (Figure 2.13). Fruit set was substantially higher following intermorph pollination (100%) than selfing or intramorph pollination (Figure 2.13). There was no variation between the populations ($\chi^2 = 0.08$, df = 1, $P = 0.781$). No two-way interactions were significant ($P > 0.419$).

The results of the split-plot ANOVA on hand-pollinated seed set demonstrated that the number of mature seeds per fruit depended significantly on pollination treatments and the interaction between population and morph (Table 2.8). The L-morphs showed strong self- and intramorph incompatibility and only intermorph pollination resulted in seed set in both populations (Figure 2.14; 65.9 mature seeds per fruit following intermorph pollination). According to the Lloyd and Schoen (1992) index the L-morphs were highly self-incompatible in both populations (DD: SII = 0.015 and TL: SII = 0.032). The S-morphs, however, showed partial self-incompatibility in both populations (Figure 2.14; DD: SII = 0.066 and TL: SII = 0.328). Ten percent of the S-morph plants in the TL population were highly self-compatible with indices greater than 0.855. Following intermorph pollination, the S-morphs produced 73.3 mature seeds per fruit (Figure 2.14).

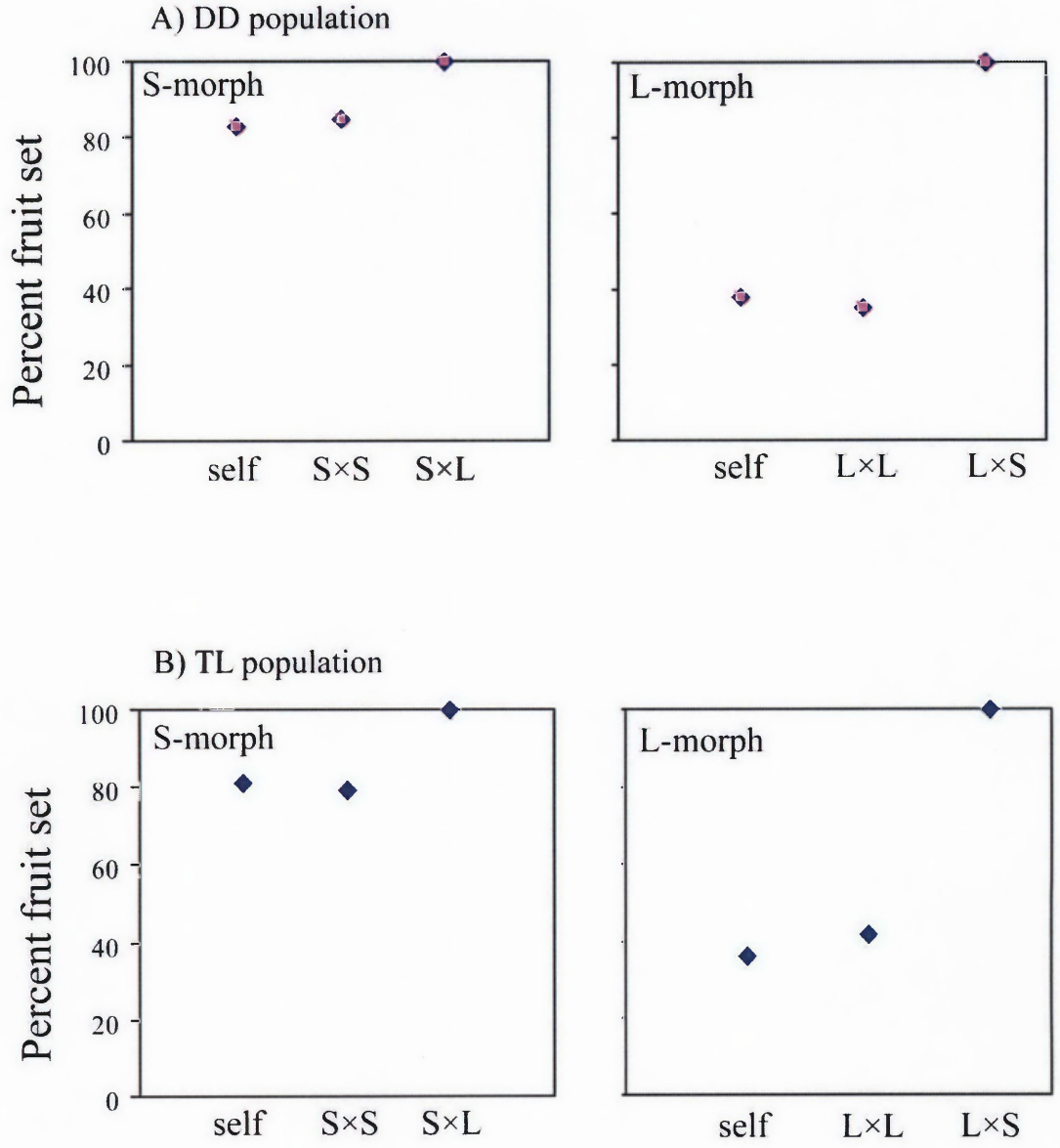

Figure 2.13. Results of the hand-pollinated fruit set for the S-morphs (S) and the L-morphs (L) of *Nymphoides montana* from A) Dumaresq Dam (DD) and B) Thomas Lagoon (TL) populations. Mean percent fruit set following self, intramorph (S×S or L×L) and intermorph (S×L or L×S) pollinations is given. The S-morphs produced greater numbers of fruits following both self- and intramorph pollinations than the L-morphs. Both morphs showed high fruit set following intermorph pollination.

Table 2.8. Results of the split-plot ANOVA to test the effects of population, plant, morph and pollination treatment on hand-pollinated seed set in *Nymphoides montana*. The number of mature seeds per fruit depended significantly on pollination treatments and the interaction between population and morph.

Source	Type III *SS*	df	*MS*	*F*	*P*
Between subject factors					
Population	289.60	1	289.60	2.28	0.356
Morph	194.25	1	194.25	1.66	0.416
Population × morph	121.65	1	121.65	5.03	0.028
Plant (population and morph)	1460.01	61	23.93	0.94	0.603
Within subject factors					
Pollination treatment	21391.07	2	10695.54	320.52	0.003
Population × pollination treatment	66.91	2	33.45	1.31	0.274
Morph × pollination treatment	19.36	2	9.68	0.38	0.686
Error	2528.25	99	25.54		

F-test for the effect of population, morph, population × morph interaction and pollination treatment used a synthetic denominator mean square (*MS*). For population, the denominator was $MS_{\text{population} \times \text{morph}} + MS_{\text{population} \times \text{pollination treatment}} - MS_{\text{error}}$; for morph, the denominator was $MS_{\text{population} \times \text{morph}} + MS_{\text{error}}$; for population × morph interaction, the denominator was $MS_{\text{plant (population morph)}} + MS_{\text{error}}$ and for pollination treatment, the denominator was $MS_{\text{population} \times \text{pollination treatment}} + MS_{\text{error}}$.

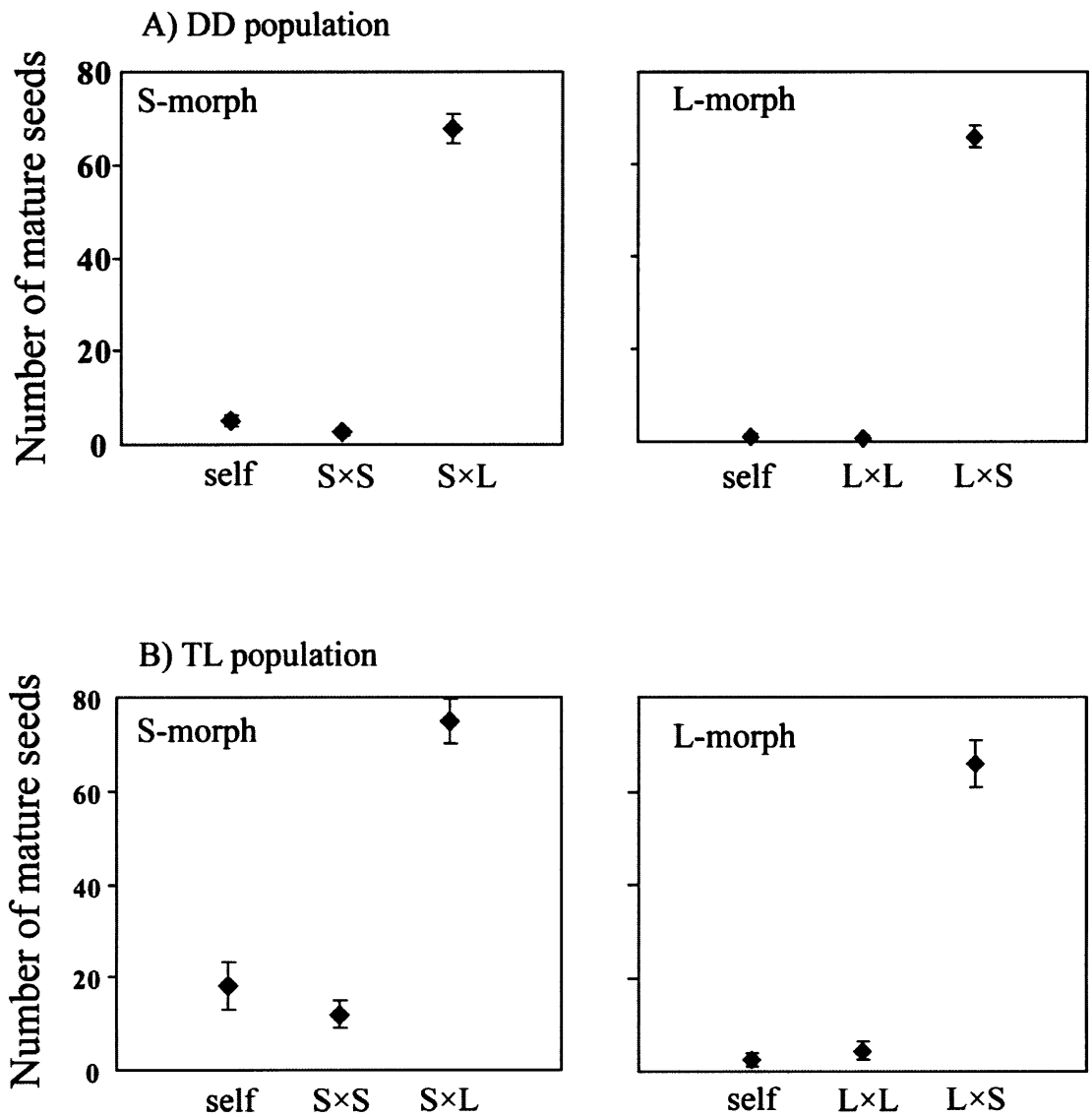

Figure 2.14. Results of the hand-pollinated seed set for the S-morphs (S) and the L-morphs (L) of *Nymphoides montana* from A) Dumaresq Dam (DD) and B) Thomas Lagoon (TL) populations. Mean (± SE) number of mature seeds following self, intramorph (S×S or L×L) and intermorph (S×L or L×S) pollinations is given. Both morphs are predominantly self- and intramorph incompatible. However, in one population (TL), self- and intramorph incompatibility of the S-morphs was weaker than those of the L-morphs with 10% of the plants being strongly self-compatible.

2.4.7 Autonomous self-fertilisation

The results of the analysis of deviance on autonomous fruit set showed that both populations and morphs differed significantly (population: $\chi^2 = 25.05$, df = 1, $P < 0.0001$; morph: $\chi^2 = 20.92$, df = 1, $P < 0.0001$). For the L-morphs, no flowers set fruit in the DD population and only 4% of the flowers set fruit in the TL population. However, for the S-morphs, 10% of the flowers in the DD population set fruit compared with 50% of the flowers in the TL population.

For the L-morphs, an average of one seed per fruit was produced in both populations. For the S-morphs, mean seed set in the TL population was over four times greater than that for the DD population (TL: 5.68 ± 2.35 and DD: 1.25 ± 0.25). The difference in the seed set between the two populations was marginally significant (t-value= − 1.87, df = 9, P-value = 0.094). The AFI indices for the S-morphs were 0.038 and 0.002 in the TL and DD populations, respectively. Ten percent of the S-morph plants in the TL population, the same plants with SII > 0.855, showed indices greater than 0.222.

2.4.8 Open pollinations

In 2005, percent fruit set of both morphs was greater than 68% in both populations under natural conditions (Table 2.9). There was no significant difference in open-pollinated fruit set between the populations and the morphs (population: $\chi^2 = 2.61$, df = 1, $P = 0.106$; morph: $\chi^2 = 9.83$, df = 1, $P = 0.754$). The morph × population interaction was also not significant ($\chi^2 = 0.19$, df = 1, $P = 0.662$). In 2007, however, natural pollinations resulted in lower fruit development for the L-morphs (50%) *vs.* the S-morphs (84%; $\chi^2 = 8.78$, df = 1, $P = 0.003$).

In 2005, percent seed set of both morphs was greater than 71% in both populations (Table 2.9). The effect of morph was marginally significant in the DD population (one-way ANOVA; $F_{1,80} = 2.92$, $P = 0.091$). There was no significant difference in the seed set between the morphs in the TL population (one-way ANOVA; $F_{1,59} = 0.05$, $P = 0.829$). In the DD population in 2007, however, the S-morph fruits had fewer seeds than fruits of the L-morphs (Table 2.9; $F_{1,45} = 10.45$, $P = 0.002$).

Comparing 2005 and 2007 in the DD population, the number of S-morph ovules that developed into seeds reduced significantly from year to year (one-way ANOVA; $F_{1,69} =$

8.09, *P*-value = 0.006). The effect of year was not significant in the L-morphs ($F_{1,56}$ = 1.23, *P*-value = 0.272).

Table 2.9. Results of the two-year open-pollinated experiment showing mean fruit set and seed set (± SE) of the S-morphs and the L-morphs of *Nymphoides montana* in the Dumaresq Dam (DD) and Thomas Lagoon (TL) populations. No data were available from the TL population in 2007. In the DD population, the number of S-morph ovules that matured into seeds reduced significantly from 2005 to 2007.

Year/population/morph	No. of open-pollinated flowers	% fruit set per flower	No. of mature fruits	% seed set per ovule
2005				
DD				
S-morph	38	84.2	47	82.8 ± 4.9
L-morph	34	79.4	34	71.2 ± 6.1
TL				
S-morph	22	68.1	31	74.9 ± 4.9
L-morph	23	69.5	30	73.4 ± 4.4
2007				
DD				
S-morph	31	83.8	24	60.0 ± 5.5
L-morph	40	50.0	24	81.1 ± 6.0

2.5 Discussion

The first thing that defined *Nymphoides montana* as a distylous species was its segregation into two discrete floral morphs that differed reciprocally with respect to the stigma and anther heights (Figure 2.8), as reported in other species (Ganders 1979; Barrett 1990; Lloyd and Webb 1992a; Richards and Koptur 1993; Thompson *et al.* 1998; Faivre and McDade 2001). Distyly was also associated with self- and intramorph incompatibility systems (Figure 2.13, Figure 2.14), a 1:1 morph ratio (Table 2.2) and a suite of ancillary dimorphic traits. Pollen grain size and corolla tube length were consistently greater in the S-morphs (Table 2.7, Table 2.4), whereas the L-morphs produced larger stigmatic papillae and more pollen with smoother exine sculpture (Table 2.7 Figure 2.11, Figure 2.12). However, *N. montana* exhibits some aspects of an atypical distyly syndrome, including partial incompatibility of the S-morphs and a weak reciprocity between the long-level sex organs.

2.5.1 Morph ratio and reproductive success

The study populations of *Nymphoides montana* showed no deviations from an equal morph ratio in the first study year. However, the L-morphs were more abundant than the S-morphs in the DD population in the second study year, whereas the floral morphs were equally represented in the GC population (Table 2.2). The occurrence of populations with a 1:1 morph ratio indicates that the morphs are maintained by disassortative mating (Arroyo and Barrett 2000). Unequal morph ratios can result from self- and intramorph compatibility, differences in clonal propagation, flowering and survival between floral morphs, and historical factors (Pailler and Thompson 1997; Thompson *et al.* 1998). In the present study, the morph ratio was determined toward the end of flowering season, and there was a tendency toward a greater numbers of the L-morphs in all the study populations. Therefore, the deviation from a 1:1 morph ratio could result from differences in mortality or growth form and size of clones between the morphs. In *Menyanthes trifoliata*, Thompson *et al.* (1998) suggested that historical factors, such as effect of waterfowl in seed dispersal, may cause unbalanced morph ratios within populations.

In *Nymphoides montana*, the reproductive success of the floral morphs was high in the two populations with equal morph ratios (DD, TL) in the first study year. This indicates

the two morphs were spatially well mixed, and they received sufficient compatible pollen despite the observed differences in the number of plants (population size = 142–2,469) and the distance between the plant morphs (population density = 0.05–0.67 m^2) of each study sites. In the second study year, however, fruit set of the L-morphs was reduced in the biased population (DD), probably as a result of a shortage of S-morphs and compatible pollen in a few clumped patches of the L-morphs. Therefore, there was a greater chance for illegitimate pollinations to occur in the L-morphs. Spatial distribution of floral morphs is believed to play a key role in determining reproductive success of species with extensive clonal propagation (Shibayama and Kadono 2003; Wang *et al.* 2005; Brys *et al.* 2007). Reproductive success decreases with increasing distance between mating partners in several distylous aquatic species, such as *Nymphoides indica* (Shibayama and Kadono 2003), *N. peltata* (Wang *et al.* 2005), and *Hottonia palustris* (Brys *et al.* 2007) by reducing the availability of compatible pollen. Further study is required to assess the effects of spatial distribution of floral morphs on reproductive success in *N. montana*.

2.5.2 Between-morph variations in ancillary traits

The ancillary traits of *Nymphoides montana* are similar to those expected for typical distylous species (Ganders 1979; Dulberger 1992). Stigmas are dimorphic in size, shape and papillae morphology. The L-morph stigmas are larger than the S-morph stigmas. Dulberger and Ornduff (2000) also reported this difference for ten species of *Villarsia*. However, the stigmatic surface area appears to be greater in the S-morphs than in the L-morphs because of the higher number of stigmatic sub-lobes and the widely distributed papillae on both the interior and exterior surfaces of the stigmatic lobes. Morph differences are not always consistent in distylous species. In some distylous species S-morph stigmas are larger than L-morph stigmas, e.g., species of *Palicourea* (Sobrevila *et al.* 1983), *Luculia gratissima* (Murray 1990), *Palicourea padifolia* (Ree 1997), species of *Psychotria* (Faivre and McDade 2001) and *Psychotria nuda* (de Castro and Araujo 2004). The observed stigmatic papillae dimorphism in this study has been reported in different species of *Villarsia* (Dulberger and Ornduff 2000) and in *Primula malacoides* (Pandey and Troughton 1974) and *Linum pubescens* and *L. grandiflorum* (Dulberger 1974; Dulberger 1992).

The pollen of *Nymphoides montana* is dimorphic in size, number and exine sculpture. Pollen grain size of the S-morphs was consistently greater; Ornduff (1966) observed a

similar situation in distylous species of *Nymphoides indicia, N. humboldtiana* and *N. peltata.* However, the L-morphs produced more pollen grains per flower. Ganders (1979) suggested that, in distylous species, greater pollen production in L-morphs was a response to the less accessible stigmas of S-morphs positioned deep within the floral tubes. Alternatively, Price and Barrett (1982) suggested that morph differences in pollen production may be an outcome of morph-specific differences in floral development rather than being an adaptive feature of the flower. Pollen grain exine dimorphism is associated with distyly in *N. montana.* The pollen grain surface is smooth in the S-morphs and granular in the L-morphs; this was also observed in a number of distylous species of *Damnacanthus* (Naiki and Nagamasu 2003; Naiki and Nagamasu 2004). The observed ancillary dimorphic traits of pollen and stigma should function to promote intermorph pollen transfer by limiting stigma-pollen interference and self-fertilisation (Barrett 1992c; Lloyd and Webb 1992a; Lloyd and Webb 1992b; Dulberger and Ornduff 2000).

In *Nymphoides montana*, the S-morph flowers display larger corolla tube length and corolla tube width than those of the L-morphs. In the TL population, however, the differences in the corolla tube length between the morphs were only marginal. Larger corollas for S-morphs have been reported in several taxa, e.g. *Lithospermum caroliniense* (Levin 1968), *Amsinckia grandiflora* (Ornduff 1976), *Gaertnera vaginata* (Pailler and Thompson 1997), *Palicourea padifolia* (Contreras and Ornelas 1999) and *Bouvardia ternifolia*, *Psychotria poeppigiana* and *P. chiapensis* (Faivre and McDade 2001). Pailler and Thompson (1997) suggested that the longer corolla tube of S-morphs in distylous species may have contributed to the reciprocity of anther position because of the direct attachment of the anthers to the corollas.

2.5.3 Reduced herkogamy and weak reciprocity

By definition, plants of distylous species are of two strictly distinct floral morphs with anthers and stigmas at reciprocal heights (Ganders 1979; Barrett 1990; Lloyd and Webb 1992a; Richards and Koptur 1993; Thompson *et al.* 1998; Faivre and McDade 2001). This study also shows *Nymphoides montana* is segregated into two discrete floral morphs and can be defined as a distylous species (Figure 2.8). In this species, however, the S-morph anthers are positioned well below the L-morph stigmas, resulting in weak reciprocity of the long-level sex organs (Figure 2.9 and Figure 2.10). Indeed, the dimorphism in the anther height is less pronounced than that of the stigma height. Similar results have been

reported in different species of Menyanthaceae, such as in *Nymphoides humboldtiana, N. peltata* (Ornduff 1966), *Villarsia parnassifolia, V. capitata, V. lasiosperma* (Ornduff 1986) and *Menyanthes trifoliata* (Thompson *et al.* 1998) and other families, e.g. Rubiaceae such as in *Gaertnera vaginata* (Pailler and Thompson 1997) and *Palicourea padifolia* (Ree 1997). Lloyd and Webb (1992a) suggested that incomplete sex-organ reciprocity is associated with stronger selection to segregate the stigma positions than the selection to segregate the anther positions dutring the evolution of distyly.

2.5.4 Phenotypic correlations and traits contributing in reciprocity

The relationships among the floral traits and their effects on reciprocity were further investigated using phenotypic correlations. In *Nymphoides montana*, the stigma–anther separation is significantly correlated with the female traits of the L-morphs and with the male traits of the S-morphs. These phenotypic correlations indicate that female floral traits of the L-morphs and male floral traits of the S-morphs contribute to the degree of reciprocal herkogamy in *N. montana* (Table 2.6).

Furthermore, the matrices of the phenotypic correlations show that a greater proportion were significant for the S-morphs compared with the L-morphs. This would imply greater phenotypic integration among floral traits in the S-morphs of *Nymphoides montana*. Since the S-morph stigmas are positioned below the anthers, pollinator-mediated self-pollination is more likely to occur (Webb and Lloyd 1986; Barrett 2003). In such a floral design, phenotypic integration could increase to promote intermorph cross-pollination. Anderson and Bush (2006) suggested that the degree of phenotypic integration within a flower increases as plant-pollinator interactions become efficient at securing pollen donation and receipt. However, it appears that the within-flower integration does not minimise negative effects of self- and intramorph pollinations on the S-morph seed set in the second study year (discussed below).

2.5.5 Consequences of weak reciprocity: increased selfing and imprecise pollen transfer

In *Nymphoides montana*, the S-morph anthers are positioned at close proximity to the stigmas, and are not reciprocally positioned to the stigmas of the L-morphs (Figure 2.15). Reduced stigma–anther separation and weak reciprocity between long-level organs may

increase the likelihood of sexual interference (Lloyd and Yates 1982; Barrett 2002b) and imprecise pollen transfer (Ganders 1979), respectively.

In the S-morphs, reduced stigma–anther separation limits separation between the sites of pollen donation and deposition on the pollinator's body during its visits to the flowers (Figure 2.15). Consequently, the S-morphs could show significant reductions in fertility due to self- and intramorph pollination. Such pollinations may have contributed to the reduced open pollinated seed set of the S-morphs in the second study year (Table 2.9). It is generally accepted that self- (or incompatible) pollination has negative influences on female function by stigma clogging (Yeo 1975; Waser 1978a; Waser 1978b), pollen clogging (Ockendon and Currah 1977; Kanchan and Chandra 1980; Thomson *et al.* 1982) and ovule discounting (Yeo 1975; Shore and Barrett 1984; Broyles and Wyatt 1993; Ramsey 1995; Barrett 2002b). The effects of prior or simultaneous self-pollinations on seed set in *N. montana* needs to be investigated to elaborate the costs of self-pollination (Barrett 2002b).

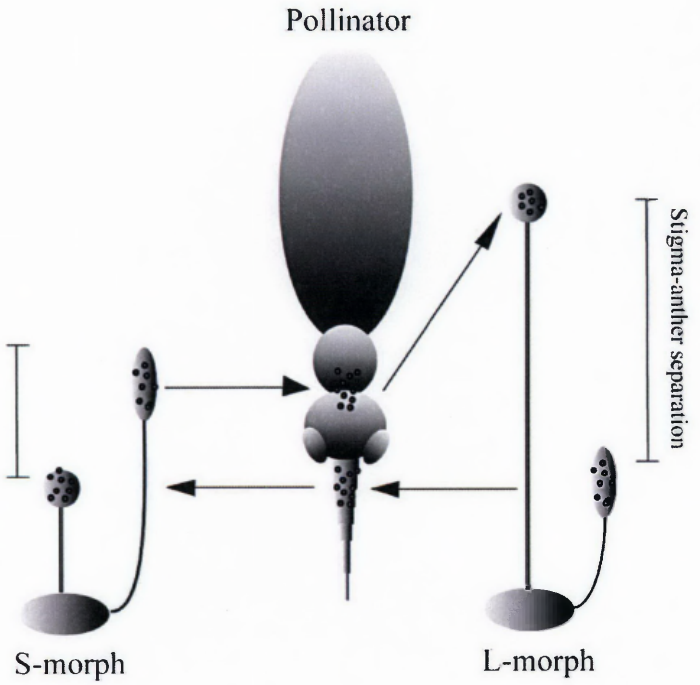

Figure 2.15. Reduced stigma–anther separation of the S-morphs and weak reciprocity between the long-level sex organs in *Nymphoides montana* may increase the likelihood of sexual interference in the S-morphs and imprecise pollen transfer toward the L-morph stigmas, respectively. Diagram modified from Sakai and Toquenaga (2004).

Reciprocal positioning of anthers and stigmas is believed to promote efficient pollen transfer, since both sexual organs from the two morphs contact similar locations of a pollinator's body (Ganders 1979; Olesen 1979; Lloyd and Webb 1992b; Stone and Thomson 1994; Barrett *et al.* 2000). Minor changes in floral morphology of distylous species, however, can significantly affect pollination efficiency (Ganders 1979; Ree 1997; Faivre and McDade 2001; Lau and Bosque 2003). For example, Ganders (1979) found that differences of as little as 1 mm in stigma and anther heights of the L-morph flowers in distylous *Lithospermum californicum* affected the level of intermorph pollination.

In *Nymphoides montana*, it was expected that the height differences between the S-morph anthers and the L-morph stigmas (Figure 2.15) would result in compatible pollen wastage and reduce the probability of successful compatible pollen deposition on the L-morph stigmas. However, almost complete fertilisation of the ovules within developing fruits of the L-morphs, with over 71% seed set, indicates that the imperfect reciprocity of sex-organ positions does not adversely affect reproductive success. Instead, the strong incompatibility systems of the L-morphs (SII < 0.032), which only allow ovule fertilisation by the S-morph pollen, are most likely to control the mating system. Measurements of pollen load on stigmas of each floral morph are required to estimate the proportion of compatible pollen deposited by pollinators (Ganders 1979; Glover and Barrett 1986; Ree 1997; Lau and Bosque 2003; Massinga *et al.* 2005).

2.5.6 Partial incompatibility and reduced herkogamy

Comparisons of the fruit and seed set following self-, intramorph and intermorph pollinations clearly demonstrate that distyly is accompanied by the presence of a diallelic incompatibility system in *Nymphoides montana* (Figure 2.13, Figure 2.14). In both S-morphs and L-morphs, self- and intramorph pollinations produce significantly less fruit and seed than cross-pollinations with pollen from anthers of an equivalent height as the stigma. However, the expression of self- and intramorph incompatibility is weaker in the S-morphs than the L-morphs. Variations in dimorphic incompatibility have been reported in several atypical distylous species of Menyanthaceae, including: a) self- and intramorph compatibility in *Nymphoides peltata* (Ornduff 1966), b) intramorph compatibility in *Villarsia calthifolia* and *V. violifolia* (Dulberger and Ornduff 2000) c) between-morph variation in intramorph compatibility in *Villarsia parnassiifolia* (Ornduff 1988), and *V. exaltata V. lasiosperma* and *V. marchantii* (Dulberger and Ornduff 2000). Other

distylous species have also shown between morph variation in the degree of incompatibility, such as *Guettarda roupalaefolia* (Ruiz Zapata and Kalin Arroyo 1978), *Gaertnera vaginata* (Pailler and Thompson 1997) and *Hottonia palustris* (Brys *et al.* 2007).

The partial self- and intramorph incompatibility of the S-morphs of *Nymphoides montana* possibly arose in conjunction with the reduced stigma–anther separation. Nearly, 10% of the S-morphs were highly self-compatible (SII > 0.855) in the population of the S-morphs with little stigma–anther separation (TL; Figure 2.10). The observed reduced herkogamy of the S-morphs and its possible association with partial self-incompatibility in this study has also been reported in *N. peltata* by Ornduff (1966). Genetic markers can be used to estimate selfing rates in the S-morph individuals with varying degrees of stigma–anther separation to determine whether there is a correlation between the floral morphology and level of self-fertilisation (Barrett and Shore 1987).

The syndrome of morphological features and incompatibility systems associated with distyly is thought to be governed by a supergene comprising a series of tightly-linked genes (Ernst 1955; Dowrick 1956; Barrett 1979; Lewis and Jones 1992; Lloyd and Webb 1992b; Richards and Barrett 1992; Kurian and Richards 1997; Richards 1997; Tamari *et al.* 2005). Each gene is responsible for various sub-characters of distyly, e.g. a pollen incompatibility reaction or stigma and anther height. On this basis, if the same linkage occurs in *Nymphoides montana*, one genetic explanation for the alteration to the length of stamens in the S-morphs and the association of this with partial incompatibility could be a system of genetic modifiers. It has been suggested that a series of modifier genes that have non-allelic associations with the heterostyly supergene reduce the flower size and length of the reproductive organs (Ornduff 1972; Barrett 1979; Shore and Barrett 1986; Ornduff 1988; Barrett and Cruzan 1994; Fenster and Barrett 1994). These floral modifications are also accompanied by relaxation or complete loss of the incompatibility system. To study whether reduced anther height is associated with pollen compatibility, pollen competition experiments using controlled crosses of modified and unmodified S-morphs are required (Manicacci and Barrett 1995).

Alternatively, in *Nymphoides montana*, the incompatibility of the S-morphs could operate independently of morphological features, as described by Ornduff (1988) for the L-morphs of *Villarsia parnassiifolia*. Morphological components are not always associated with incompatibility systems (Barrett 1992c; Barrett *et al.* 2000). For example, Dulberger

(1970) and Philipp and Schou (1981) have reported that incompatibility systems of two atypical distylous *Anchusa hybrida* and *A. officinalis*, respectively, are not tightly linked to morphological features.

2.5.7 Capacity for autonomous self-fertilisation

In *Nymphoides montana*, the S-morphs have a greater capacity for autonomous self-fertilisation than the L-morphs; this variation appears to be associated with intermorph variation in floral morphology that enhances self-pollination. In the S-morphs, the fall of senescent corollas forces the recurved stamens, positioned at the throat of the floral tube (Figure 2.1 A), to contact the stigma as the flowers close. Lloyd and Schoen (1992) suggested that the movement of the flower's parts, for example the corolla, particularly in species with epipetalous stamens, leads to pollen-stigma contacts and self-pollination at the end of the flowering day. In the L-morphs, however, less pollen is captured by the stigmas before the flowers close because the stigmas are extended beyond the anthers (Figure 2.1 B).

Furthermore, the ability of the S-morphs to self-fertilise autonomously varied between the populations (10–50% fruit set). In the TL population, the self-compatible plants of the S-morphs were also able to set full seed through unmanipulated self-pollination (AFI > 0.222). Autonomous seed production is known as an adaptation to insufficient pollinator service (Ramsey *et al.* 1993; Fausto *et al.* 2001; Kalisz and Vogler 2003; Totland and Schulte-Herbrüggen 2003). The high levels of open-pollinated fruit and seed set in the populations studied, however, indicate abundant pollinator activity. Comparative studies of the relationship between pollinator visitation rate and the ability to self-pollinate and fertilise at the population level are required to test this hypothesis explicitly.

2.6 Conclusions

The typical distylous features of *Nymphoides montana* are self- and intramorph incompatibility, reciprocal herkogamy, strong pollen and stigma dimorphism and a 1:1 morph ratio in populations. *N. montana* is, however, atypical in the degree of reciprocity between the long-level sex organs and the incompatibility systems of the S-morphs. Imperfect reciprocity and partial incompatibility are usually implicated in evolutionary transitions to, or from, the distylous breeding system. In this study, however, other lines of

evidence indicate the maintenance of distyly in the *N. montana* populations during the years studied. Floral visitors were active and both morphs produced a high number of fruits and seeds in the natural populations. In most cases, where, for example, a breakdown of distyly has occurred, alteration in stigma and anther position (or weak reciprocity) has accompanied complete self-compatibility (Riveros *et al.* 1987; Barrett 1989a; Richards and Koptur 1993). In *N. montana*, however, self-incompatibility was strongly presented in the L-morphs but only partial in the S-morphs. Also, an evolutionary breakdown of distyly is usually reflected by unbalanced morph frequencies within a population (Barrett *et al.* 2000). In two of the three populations studied, however, the floral morphs presented in equal ratios (1:1) and had equivalent open-pollinated fruit set, indicating each morph can only mate with the opposite mating partner. Further studies are required to determine definitely that distyly is maintained and, more specifically, to examine the functionality of distyly in the study populations. Measurements of stigmatic pollen loads, for example, are required to record the magnitude of compatible *vs.* incompatible pollen flow in the natural populations (Ganders 1979; Lau and Bosque 2003; Ornelas *et al.* 2004; Massinga *et al.* 2005).